uppermost Eocene to lowermost Miocene of the western North Atlantic (IODP **Expedition 342, Paleogene Newfoundland sediment drifts)** Lisa M. Egger^{a*}, Katarzyna K. Śliwińska^b, Tim E. van Peer^c, Diederik Liebrand^c, Peter C. Lippert^d, Oliver Friedrich^a Paul A. Wilson^c, Richard D. Norris^e, Jörg Pross^a ^a Institute of Earth Sciences, Heidelberg University, Im Neuenheimer Feld 234, D-69120 Heidelberg, Germany ^b Geological Survey of Denmark and Greenland (GEUS), Øster Voldgade 10, DK-1350 Copenhagen K, Denmark ^c National Oceanography Centre, University of Southampton, Waterfront Campus, European Way, Southampton SO14 3ZH, UK ^d Department of Geology and Geophysics, University of Utah, Frederick A. Sutton Building, 115 S 1460 E, Salt Lake City, UT 84112, USA ^e Scripps Institution of Oceanography, University of California, San Diego, 9500 Gilman Drive, La Jolla, CA 92093-0244, USA Corresponding author: Lisa M. Egger, phone: +49 (0)6221-54 4830, e-mail: lisa.egger@geow.uni-heidelberg.de

Magnetostratigraphically-calibrated dinoflagellate cyst bioevents for the

Abstract

28

29

30

31

32

33

34

35

36

37

38

39

40

41

42

43

44

45

The Oligocene epoch represents a somewhat neglected chapter in paleoclimate and paleoceanographic history, which is at least partially due to the scarcity of complete Oligocene sedimentary archives and poor biostratigraphic age control. Many of the biotic events registered in Oligocene microfossils are strongly diachronous across latitudes as a response to increased global cooling and enhanced meridional temperature gradients. To improve biostratigraphic age control for the Oligocene of the North Atlantic Ocean, we carried out a high-resolution study of dinoflagellate cysts from Integrated Ocean Drilling Program (IODP) Sites U1405, U1406 and U1411 off Newfoundland. Together the sites comprise an apparently complete uppermost Eocene (34.9 Ma) to lowermost Miocene (21.7 Ma) sequence with good magnetostratigraphic age control. This allows us to firmly tie identified dinoflagellate cyst bioevents to the geomagnetic polarity timescale. In the dinoflagellate cyst assemblages studied we have identified and magnetostratigraphically-calibrated ten first and 19 last appearance datums. Our magnetostratigraphically-calibrated dinocyst-based biostratigraphy, which is based on an average sample resolution of a sample every ~150 kyrs, will contribute to an improved age framework for future paleoceanographical studies in the higher-latitude North Atlantic.

46

47

48

Keywords: Paleogene; Oligocene; biostratigraphy; dinoflagellates; North Atlantic; Integrated Ocean Drilling Program

49

50

51

52

53

54

55

1 Introduction

Positioned between the early Paleogene greenhouse and the well-developed

Neogene icehouse worlds, the Oligocene epoch (33.9–23.03 Ma; Gradstein et al.,

2012) represents in many ways the neglected 'middle child' of Cenozoic

paleoceanography and paleoclimatology (Shipboard Scientific Party, 2002). This

status has at least partially resulted from the sparseness of complete Oligocene

sedimentary archives. Shelfal sequences of Oligocene age often exhibit hiatuses caused by sea-level fluctuations that reflect the waxing and waning of Antarctic ice sheets (Miller et al., 1991; Wade and Pälike, 2004; Pälike et al., 2006). Likewise, deep-marine Oligocene sequences, which would have remained largely unaffected by sea-level dynamics directly, are often fragmentary due to the onset of strong bottom-water circulation near the Eocene/Oligocene boundary (Miller and Tucholke, 1983; Davies et al., 2001). Notwithstanding these limitations, the Oligocene deserves further attention from the paleoclimatic community because it represents one of the most interesting episodes in the evolution of Cenozoic climates. Studying the Oligocene allows one to decipher the processes underlying the transition from a climate state characterized by the lack of large-scale ice sheets and associated sealevel dynamics to a climate state characterized by a unipolar glaciation, pronounced, glacially induced sea-level oscillations and the establishment of a quasi-modern oceanic circulation regime (e.g., Coxall et al., 2005; Pälike et al., 2006; Zachos et al., 2008).

Disentangling the causal mechanisms behind the long-term climate evolution and short-term dynamics in Earth's history critically hinges on the availability of highly resolved, integrated stratigraphies (e.g., Kuiper et al., 2008). Despite the enormous progress in the development of geochemical and cyclostratigraphical approaches over the past decades, microfossil-based biostratigraphy has remained an indispensable stratigraphic tool both in academic research and industry applications (e.g., Beaudoin and Head, 2004; Coccioni et al., 2008; Tauxe et al., 2012; Jenkins, 2013). However, although individual marine plankton taxa occur across vast regions, their distribution is strongly influenced by water-mass or other oceanographic boundaries (Lazarus, 1983). Hence, as a response to increased global cooling and enhanced meridional temperature gradients from the late Eocene onwards, many biotic events registered in microfossil assemblages during the Oligocene are strongly diachronous across latitudes. These diachroneities can yield substantial uncertainties

in biostratigraphic age control, thereby compromising long-distance correlations. For instance, the ranges of many Oligocene calcareous nannoplankton taxa differ strongly from low to high latitudes, which has resulted in the development of two widely used zonal schemes – the zonation of Martini (1971) is largely based on temperate regions, whereas that of Bukry (1973) relies on low-latitude sections. Similarly, many planktic foraminifers show constrictions in ranges through the Eocene and Oligocene (Boersma and Silva, 1991), as do radiolaria (Maurrasse, 1979), diatoms (Baldauf and Barron, 1990), and organic-walled dinoflagellate cysts (dinocysts) (Williams and Bujak 1977; Williams et al., 2004). Clearly, further improvement of biostratigraphic age control for the Oligocene is required, in particular with regard to the generation of chronostratigraphically (i.e., paleomagnetically and/or cyclostratigraphically) well calibrated, temporally highly resolved datums (Luterbacher et al., 2004).

With regard to the notorious incompleteness of Oligocene strata, the drift sediments recovered during Integrated Ocean Drilling Program (IODP) Expedition 342 off Newfoundland represent a remarkable exception to the rule. Besides spanning the entire Oligocene and being apparently complete, they exhibit sedimentation rates that are exceptionally high for deep-marine settings (up to 10.4 cm/kyr) and have allowed exquisite preservation of calcareous, silicious and organic-walled microfossils (Norris et al., 2014a). The high-quality paleomagnetic age control of the IODP Exp. 342 sites discussed here (see Section 4.2) provide an opportunity to develop an integrated biomagnetochronology for a number of microfossil groups that can be exported to the greater NW Atlantic region. This will ultimately allow for correlation of paleoceanographic events between the lower and higher latitudes.

2 Previous work on Oligocene dinocyst biostratigraphy

The backbone of microfossil-based biostratigraphy in the Oligocene is traditionally formed by calcareous plankton groups. However, the biostratigraphic utility of these

groups for the higher-latitude North Atlantic, and thereby also for correlation between higher and lower latitudes, is compromised by their diminished diversity and/or reduced preservation potential in polar to sub-polar settings (Baldauf and Barron, 1990; Lipps, 1993 and references therein). In contrast, organic-walled dinocysts are inert to chemical dissolution (albeit sensitive to oxidation), and they exhibit high species diversity in the Eocene to Oligocene of the high-latitude North Atlantic Ocean and adjacent seas (Damassa et al., 1990; Eldrett et al., 2004).

Over approximately the past 40 years, dinocyst biostratigraphy has emerged as a highly valuable tool in the age control of Oligocene successions from both shallow-marine, shelfal (e.g., Stover and Hardenbol, 1994; Van Simaeys et al., 2004; Schiøler, 2005; Śliwińska et al., 2010) and pelagic settings (e.g., Biffi and Manum, 1988; Brinkhuis and Biffi, 1993; Wilpshaar et al., 1996; Pross et al., 2010). In many cases, Oligocene dinocyst bioevents have been chronostratigraphically calibrated using information from calcareous microfossil groups, notably calcareous nannoplankton (e.g., Biffi and Manum, 1988; Head and Norris, 1989; Damassa et al., 1990; Pross, 2001; Van Simaeys et al., 2004). However, under a climate regime with strong meridional temperature gradients as was the case during the Oligocene, calcareous nannoplankton bioevents tend to be diachronous (Backman, 1987), and the preservation of calcareous nannoplankton assemblages in high-latitude settings is strongly compromised by enhanced carbonate dissolution (Berger et al., 1989; Eldrett et al., 2004).

To date, remarkably few dinocyst biostratigraphies with robust magnetostratigraphic calibration have become available for the Oligocene (Fig. 1). With the exception of the biostratigraphic data provided by Tauxe et al. (2012), Houben et al. (2013) and Peter Bijl (pers. comm.) for the high-latitude Southern Ocean, they are exclusively based on successions from the Northern Hemisphere (Fig. 2). Lower-latitude information from the Northern Hemisphere is primarily available from the Tethyan realm. Based on material from the Umbria–Marche region

of Central Italy, which is home to some of the most complete Oligocene successions known from the western Tethys, Brinkhuis and Biffi (1993) established a dinocyst zonation for the Eocene/Oligocene transition interval. Subsequently, Wilpshaar et al. (1996) extended this work into younger strata, generating a dinocyst zonation for the entire Oligocene. Their conclusion that this zonation could be used throughout the Mediterranean region was later confirmed by Peeters et al. (1998) and Torricelli and Biffi (2001). Integrating higher-resolution datasets from different sections in the Umbria-Marche Basin, Coccioni et al. (2008) and Pross et al. (2010) further refined the chronostratigraphic calibration of Oligocene dinocyst bioevents for the Tethyan realm.

Mid-latitudinal, magnetostratigraphically-calibrated dinocyst bioevents for the Oligocene are primarily known from the North Sea Basin (Fig. 1). Śliwińska et al. (2012) established an integrated bio- and magnetostratigraphy for the Rupelian and Chattian based on onshore deposits from Denmark. Dybkjær et al. (2012) studied the Oligocene-Miocene boundary interval, and Thomsen et al. (2012) presented a magnetostratigraphic calibration for some of the Eocene to earliest Oligocene bioevents previously identified by Heilmann-Clausen and Van Simaeys (2005). A cross-calibration of magnetostratigraphic and dinocyst biostratigraphic data for part of the lower Rupelian of the northern Alpine Foreland basin in Southern Germany has been carried out by Kempf and Pross (2005).

For the higher-latitude North Atlantic, a wealth of magnetostratigraphically-calibrated dinocyst data has become available from Deep-Sea Drilling Project (DSDP) Site 338 and Ocean Drilling Program (ODP) Sites 643 and 913 in the Norwegian–Greenland Sea (Fig. 2; Eldrett et al., 2004; Eldrett and Harding, 2009). Following up on the previous, low-resolution work of Manum (1976), Eldrett et al. (2004) developed magnetostratigraphies for the middle Eocene to lower Oligocene (Chrons C21r to C12n) of DSDP Site 338 as well as ODP Sites 319B and 643A; they identified numerous dinocyst bioevents for this time interval. An account of Eocene

dinocyst events at DSDP Site 338 was later presented by Eldrett and Harding (2009); this study also straddles the Eocene/Oligocene boundary. For ODP Site 647 in the Labrador Sea, Firth et al. (2012) established an integrated, early to late Eocene magneto- and multi-microfossil-group biostratigraphy that also yielded a number of dinocyst bioevents. They utilized some of the dinocyst datums previously magnetostratigraphically calibrated by Eldrett et al. (2004) in their identification of magnetic reversals. Depending on the interpretation of the paleomagnetic signals obtained, the ODP Site 647 record extends into the early or 'middle' Oligocene (Chrons C13r or C9n). Firth et al. (2012) also re-examined the original work on ODP Site 647 dinocysts of Head and Norris (1989).

Here we present magnetostratigraphically-calibrated dinocyst bioevents from the latest Eocene to earliest Miocene successions off Newfoundland that were drilled in 2012 during IODP Expedition 342 ('Paleogene Newfoundland Sediment Drifts'). The cores recovered during IODP Expedition 342 have yielded the first stratigraphically apparently complete record of the entire Oligocene in the higher-latitude Northwest Atlantic (Norris et al., 2014a). As such, and considering the high-quality magnetostratigraphical age control for the material (Norris et al., 2014a, Van Peer et al., in press), they can provide a future reference record for the greater Northwest Atlantic region, with the potential of exporting the magnetostratigraphically-calibrated biostratigraphical datums identified from their dinocyst assemblages to the higher-latitude North Atlantic. Ultimately, our study aims to establish a chronostratigraphic framework for future paleoenvironmentally- and paleoceanographically-oriented research on the Oligocene of the higher latitudes of the Northern Hemisphere.

3 Studied sites

The successions analyzed in this study have been recovered during IODP Expedition 342 from drift-sediment deposits ca. 700 km east-southeast of Newfoundland (Fig.

2). IODP Expedition 342 was designed to recover Paleogene sedimentary sequences with exceptionally high sedimentation rates, with the overarching goal of reconstructing the evolution of the carbonate compensation depth in the North Atlantic during the Paleogene. The Oligocene sequences have sedimentation rates of 1.5 to 10 cm/kyr (Norris et al., 2014a). Owing to these high sedimentation rates and the relatively high clay content of the sediments, calcareous, siliceous and notably organic-walled microfossils are unusually well preserved in much of the IODP Expedition 342 core material (Expedition 342 Scientists, 2012).

196

197

198

199

200

201

202

203

204

205

206

207

208

209

210

211

212

213

214

215

216

217

218

219

220

221

222

Because of their position in the Northwest Atlantic Ocean offshore Newfoundland, the IODP Expedition 342 drillsites provide archives of information on two different surface-water regimes, i.e., the (proto-) Gulf Stream and the (proto-) Labrador Current. For the studied time interval, there is no conclusive evidence about North Atlantic surface-water patterns. While the existence of the Gulf Stream is relatively well established from at least the early Miocene onwards (Pinet et al., 1981; Wade et al., 2001), the timing of the onset of the Labrador Current is a matter of ongoing debate, ranging from the Maastrichtian to the middle Miocene (Nederbragt, 1992; Via and Thomas, 2006; Kender and Kaminski, 2013). The presence of icerafted debris in the Arctic Sea since 46 Myr (St. John, 2008; Stickley et al., 2009) indicates seasonal sea-ice formation that might have exported fresh water to the lower latitudes via the (proto-) Labrador Current, suggesting that this current had likely been established by that time. Given this paleoceanographic setting, the successions from the studied sites allow reconstruction of the interplay between cold water-masses derived from the Labrador Sea and warm-water masses derived from the (sub-) tropical Atlantic.

During the Oligocene, the region off Newfoundland was situated at a paleolatitude of ~40°N (Norris et al., 2014a). The Oligocene succession was deposited in a deep-water sediment drift setting, with paleo-waterdepths ranging from

approximately 2800 to 4000 m (Expedition 342 Scientists, 2012). The drift sediments likely originate from the Labrador margin and the Labrador Sea (Norris et al., 2014a). Successions from three IODP Expedition 342 sites were analyzed (Sites U1405, U1406, and U1411; Fig. 2). Together, these sequences span the entire Oligocene, including the Eocene-Oligocene and Oligocene-Miocene boundary intervals. The correlation between the records from different sites was achieved using magnetostratigraphic data (Norris et al., 2014b, c, d; Van Peer et al., in press). The stratigraphical, lithological and paleoceanographical characteristics of the investigated sites with particular reference to the sampled intervals are briefly discussed in the following. From Site U1405 (coordinates: 40°08.30′N, 51°49.20′W; Fig. 2), we report dinocyst data from the latest Oligocene (Chron C6Cr) to earliest Miocene (Subchron C5Cn.1n). The site is situated on the J-Anomaly Ridge at a present-day water depth of 4285 m. During the Oligo-Miocene, greenish-grey clays to oozes were deposited that are characterized by varying abundances of radiolarians, diatoms and calcareous nannofossils. The carbonate content of these sediments ranges from 0 to 30 %. Across the Oligocene-Miocene transition there are several pale, carbonate-rich layers exhibiting high abundances of the nannofossil Braarudosphaera. Sedimentation rates based on the age model for Site U1405 (Norris et al., 2014b) are on the order of 10 cm/kyr across the studied interval. These exceptionally high sedimentation rates suggest an intensification of boundary-current flow strength and sediment transport, indicating a significant increase in drift development (Norris et al., 2014b). Site U1406 (coordinates: 40°21.0′N, 51°39.0′W; Fig. 2) is also located on J-Anomaly Ridge at a present-day water depth of 3813 m. The sedimentary sequence recovered spans the Paleocene to early Miocene. Lithologically, the Oligocene succession at Site U1406 consists of carbonate-rich nannofossil ooze in the lowermost Oligocene that is overlain by ~180 m thick brown to green nannofossil

223

224

225

226

227

228

229

230

231

232

233

234

235

236

237

238

239

240

241

242

243

244

245

246

247

248

249

250

ooze representing the early Oligocene to early Miocene. Sedimentation rates at Site U1406 during the Oligocene are between 1.0 and 3.2 cm/kyr and thus generally lower than at the deeper sites (e.g., Site U1405). This suggests that Site U1406 represents a shallower part of the J-Anomaly drift sequence that was less strongly affected by sedimentation induced by the deep western boundary-current-induced sedimentation (Norris et al., 2014c).

Located on the Southeastern Newfoundland Ridge at a present-day water depth of 3300 m, Site U1411 (coordinates: 41°37.1′N, 49°00′W; Fig. 2) recovered a late Eocene (Chron C15n) to early Oligocene (Chron C8r) succession comprised primarily of silty clay, clay with nannofossils, and silty nannofossil clay (Norris et al., 2014d). More carbonate-rich nannofossil ooze is only present immediately above the Eocene/Oligocene boundary, probably representing the widespread carbonate overshoot observed at other Expedition 342 sites (Norris et al., 2014d). Eocene and Oligocene sedimentation rates at Site U1411 are ~1.5 cm/kyr on average. Even higher values occur at the Eocene-Oligocene boundary interval (up to 3.2 cm/kyr). These generally increased sedimentation rates from the middle Eocene onwards reflect the onset of drift sedimentation at the Southeastern Newfoundland Ridge (Norris et al., 2014d).

4 Material and methods

4.1 Sampling strategy

The investigated samples from the Oligocene Expedition 342 splice comprise cores from Sites U1411 (Eocene/Oligocene transition interval; reversal C13r/C15n to C12r/C13n), U1406 (early to late Oligocene; C12r/C13n to C6Cn.3n/C6Cr), and U1405 (Oligocene/Miocene transition interval; C6Cn.3n/C6Cr to C6AAr.3r). The splice has been developed based on shipboard magnetostratigraphic and biostratigraphic (planktic foraminiferal, calcareous nannoplankton and radiolarian) data (Norris et al., 2014b, c, d). Site U1405 was sampled from Sections U1405A-

10H-6W to U1405B-21H-3W (127.70–247.39 m CCSF-A [Core Composite Depth below Sea Floor]), Site U1406 from Sections U1406A-10H-1W to U1406A-22H-4A (96.91–239.33 m revised CCSF-A, Van Peer et al., in press), and Site U1411 from Sections U1411B-15H-4A to U1411C-12X-4A (135.31–188.43 m CCSF-A). A list of all studied samples is available as Online Supplementary Material accompanying this paper.

To achieve a targeted average temporal resolution between 100 and 150 kyrs, sampling distances were calculated following the sedimentation rates as indicated by shipboard stratigraphic work. This procedure resulted in twelve samples for the Eocene/Oligocene transition interval of Site U1411, 69 samples for the early to late Oligocene interval of Site U1406, and 13 samples for the Oligocene/Miocene transition interval of Site U1405. An additional 18 samples were examined to cover a hiatus and slumping structures at Site U1406 (Van Peer et al., in press). These samples were taken from the splice for Site U1411 (from Cores U1411B-4H-6W to U1411B-10H-6W, 27.55–87.6 m CCSF-A respectively). The revised depth for samples from Site U1406 is given as revised CCSF-A (Van Peer et al., in press).

4.2 Magnetostratigraphical age control

For the magnetostratigraphic calibration of dinocyst bioevents, the shipboard-measured magnetic polarity zones were used for all samples from Sites U1411 and U1405 (compare Norris et al., 2014b, d). For Site U1406, the positions of some reversals have been modified during post-cruise research by Van Peer et al. (pers. comm.), and we have applied this updated stratigraphy wherever available.

The magnetostratigraphical reversal ages are based on the time scale of Gradstein et al. (2012). For the Oligocene the GTS2012 ages are primarily based on the astronomical tuning of ODP Site 1218 (Pälike et al., 2006). Correlation of individual polarity chrons to the geomagnetic polarity time scale was through shipboard biostratigraphical data and the identification of the magnetochron reversal pattern

(Norris et al., 2014a; Van Peer et al., in press). Biostratigraphic ages are determined from the relative position of dinocyst datums within the respective magnetochrons and given in percentages above the base of magnetochrons.

310

311

312

313

314

315

316

317

318

319

320

321

322

323

324

325

326

327

328

329

330

331

332

333

334

307

308

309

4.3 Palynological sample preparation and evaluation

In total, 113 samples were investigated for their dinocyst assemblages. The sampling strategy yielded an average temporal resolution on the order of 150 kyrs. Sample processing followed standard palynological techniques (e.g., Pross, 2001). Between 9 and 31 g of dry sediment were processed per sample. All samples from Sites U1405 and U1411, and 52 samples from Site U1406 were digested using 33 % hydrochloric acid (HCl) and 40 % hydrofluoric acid (HF); sieving was through a 15 µm nylon mesh. The residues were stained with 1% safranin (C₂₀H₁₉ClN₄), and one to five strew mounts were prepared per sample using glycerine jelly as a mounting medium. A slightly modified protocol was followed for a sample subset comprising 17 samples from Site U1406. After HCl and HF treatment, these samples were swirled in order to increase the concentration of palynomorphs, and the residues were sieved through an 11 µm mesh. Finally, all samples were briefly oxidized with potassium hydroxide (KOH, 5%). At least one strew-mount slide was prepared per sample by mounting the residue in glycerol jelly. A visual inspection of strew-mount slides obtained through the different processing protocols revealed no systematic differences in palynomorph preservation, with the exception of the stained material being easier to count and photograph.

Whenever possible, a minimum of 300 (mean: 339) dinocysts were counted per sample and identified to the species level; only in one sample less than 250 dinocysts were counted. To detect rare taxa that had not been registered during regular counts, at least one additional slide was scanned for each sample. Selected taxa were documented through photomicrographs using a Zeiss Axiocam105 color camera mounted to a Zeiss Scope.A1 light microscope. With the exception of the

sample subset from Site U1406, which is stored at the Geological Survey of Denmark and Greenland in Copenhagen, Denmark, all material is housed in the collection of the Institute of Earth Sciences, University of Heidelberg, Germany. If not stated otherwise, the dinocyst taxonomy follows Fensome and Williams (2004).

5 Results and discussion

All examined samples from the uppermost Eocene to lowermost Miocene of IODP Sites U1405, U1406 and U1411 yielded rich, exceptionally well and mostly three-dimensionally preserved palynomorph assemblages. The assemblages are dominated by dinocysts, but also contain lower numbers of (predominantly bisaccate) pollen grains and spores. Acritarchs are generally common, but reach exceptionally high abundances in a number of late Rupelian samples from Site U1406. The dinocyst assemblages are highly diverse; 110 taxa were identified (see Appendix for a full list of taxa).

5.1 Magnetostratigraphic calibration of dinocyst datums

The dinocyst assemblages contain numerous age-diagnostic marker taxa for the latest Eocene to earliest Miocene that have been described previously from the North Atlantic (e.g., Head and Norris, 1989; Williams and Manum, 1999; Eldrett et al., 2004; Fensome et al., 2009; Firth et al., 2012), the North Sea (e.g., Bujak and Mudge, 1994; Heilmann-Clausen and Van Simaeys, 2005a), and the Tethys (e.g., Wilpshaar et al., 1996; Van Mourik and Brinkhuis, 2000; Pross et al., 2010). Semiquantitative range charts are presented in Figs. 3–6. An integrated scheme of the magnetostratigraphically-calibrated dinocyst bioevents is given in Fig. 7. All ages given refer to the 2012 time scale (Gradstein et al., 2012).

The Eocene-Oligocene transition as defined by the extent of Chron C13

(Gradstein et al., 2012) is characterized by the Last Appearance Datums (LADs) of
Areosphaeridium diktyoplokum, Charlesdowniea clathrata, Cordosphaeridium cf.

funiculatum, Hemiplacophora semilunifera, Lophocysta sulcolimbata, Schematophora speciosa, and Stoveracysta sp. 1. First Appearance Datums (FADs) within that interval include those of Chiropteridium galea, Chiropteridium Iobospinosum, Filisphaera filifera, Melitasphaeridium asterium, Spiniferites manumii, and Svalbardella spp. (Figs. 3-6). The middle part of the Rupelian from Chron C12 onwards is marked by the LADs of Enneadocysta pectiniformis, S. manumii, and Phthanoperidinium comatum, as well as the FADs of Hystrichokolpoma pusillum and Oligokolpoma galeottii Pross et al., 2010. The Chattian exhibits only a few dinocyst bioevents; these are the LADs of Areoligera semicirculata, Saturnodinium pansum, and Wetzeliella spp.. The Oligocene-Miocene boundary interval as defined by the extent of Chrons C6C and C6B is marked by the LADs of *Deflandrea* spp., *F. filifera*, H. pusillum, and Svalbardella spp, and the FAD of Artemisiocysta cladichotoma (Figs. 3-7). Detailed characterizations of all registered dinocyst bioevents (FADs and LADs) are provided below in ascending stratigraphic order. A stratigraphically arranged compilation of magnetostratigraphically-calibrated FADs and LADs as they are known from different ocean basins is provided in Tables 1 and 2, respectively. We reiterate that all ages given refer to the time scale of Gradstein et al. (2012); this also applies to the dates derived from previously published papers, which have been recalculated accordingly to the Gradstein et al. (2012) timescale. The positions of the individual dinocyst events with regard to the Calcareous Nannoplankton Zones as identified in the Expedition 342 cores (Norris et al., 2014c) are also indicated.

384

385

363

364

365

366

367

368

369

370

371

372

373

374

375

376

377

378

379

380

381

382

383

5.1.1 LAD of Schematophora speciosa

- 386 *Core position:* U1411B-18H-2A, 164.43 m CCSF-A.
- 387 *Magnetostratigraphic calibration:* 69 % from the bottom of Chron C13r.
- 388 Position with regard to calcareous nannoplankton zonation: NP21.
- 389 Age assignment: 34.1 Ma.

Discussion: On the Scotian Margin off southeastern Canada, Schematophora speciosa has previously been described to have a late Eocene (middle Priabonian) LAD (Fensome et al., 2009), which is in agreement with our findings. Other than on the Scotian Margin, the taxon has not been registered previously in the North Atlantic. In the Mediterranean region, the LAD of S. speciosa occurs at the top of the Schematophora speciosa Interval Zone, which is calibrated to Chron C13r and the basal part of NP21 (Brinkhuis and Biffi, 1993). Hence, the region-specific LADs of S. speciosa appear to be quasi-synchronous in the western North Atlantic and the western Tethys.

5.1.2 LAD of Cordosphaeridium cf. funiculatum

- *core position:* U1411C-9H-4A, 159.68 m CCSF-A.
- 402 Magnetostratigraphic calibration: 77 % of Chron C13r.
- 403 Position with regard to calcareous nannoplankton zonation: NP21.
- 404 Age assignment: 34.0 Ma.

Discussion: Cordosphaeridium cf. funiculatum of Biffi and Manum (1988) differs from the type material of *C. funiculatum* as described by Morgenroth (1966a) in having shorter and thicker processes. The taxon has been previously reported from the upper Eocene of the Labrador Sea (ODP Site 647) as *Cordosphaeridium* sp. cf. funiculatum. In the Labrador Sea, it occurs until the end of NP20 (Head and Norris, 1989). In the western Tethys, the taxon occurs during the lower part of NP21, which is correlative to the latest Eocene (Biffi and Manum, 1988). Our results are well in agreement with the records from the Labrador Sea and the Tethyan region. As all previous findings of *C.* cf. funiculatum are limited to the late Eocene, this taxon may represent an important supraregional marker with remarkably similar LADs in lower-latitude settings of the western Tethys and the higher-latitude western North Atlantic.

5.1.3 LAD of Hemiplacophora semilunifera

418 Core position: U1411B-17H-3A, 154.91 m CCSF-A. 419 Magnetostratigraphic calibration: 93 % of Chron C13r. 420 Position with regard to calcareous nannoplankton zonation: NP21. 421 Age assignment: 33.8 Ma. 422 Discussion: To date, Hemiplacophora semilunifera has been rarely detected 423 previously in the North Atlantic region. Head and Norris (1989) reported the species 424 from ODP Site 647 in the Labrador Sea, where it disappears by the end of NP21. For 425 central Italy, Brinkhuis and Biffi (1993) determined the LAD of *H. semilunifera* to 426 terminate their Glaphyrocysta semitecta Interval Zone of the earliest early Oligocene. 427 This zone corresponds to the middle part of NP21, and its top is assigned to the 428 lowermost part of Chron C13r. The apparently synchronous disappearance of H. 429 semilunifera in both the western North Atlantic and the Tethys indicates the high 430 stratigraphic relevance of the species. 431 432 5.1.4 FAD and LAD of Lophocysta sulcolimbata 433 Core positions: FAD: U1411C-11X-5A, 178.83 m CCSF-A; LAD: U1411B-17H-3A, 434 154.91 m CCSF-A. 435 Magnetostratigraphic calibration: 31 % of Chron C13r and 93 % of Chron C13r, 436 respectively. 437 Position with regard to calcareous nannoplankton zonation: NP 21. 438 Age assignment: 34.6 and 33.8 Ma, respectively. 439 Discussion: In our sample material, Lophocysta sulcolimbata occurs in relatively low 440 numbers, albeit repeatedly within a very short time interval of 0.8 Myr, which 441 suggests that it may represent a useful biostratigraphic marker with a remarkably 442 short range. However, previously published information on L. sulcolimbata from the 443 greater North Atlantic region does not yield a consistent picture of the taxon's range. 444 Head and Norris (1989) provided a photomicrograph of the taxon (as *Lophocysta* sp. 445 1) from ODP Site 647 in the Labrador Sea. For ODP Site 985 in the Norwegian Sea,

Williams and Manum (1999) give a FAD at 21.1 Ma, which is much later than our findings. In the Central Danish Basin, the species was observed in the upper Eocene (Heilmann-Clausen and Van Simaeys, 2005). Based on these widely divergent ranges, the FAD and LAD of *L. sulcolimbata* as identified in our samples may only be employed regionally for the Newfoundland Margin as latest Eocene events.

451

452

453

457

458

459

460

461

462

463

464

465

466

467

468

469

470

471

472

473

446

447

448

449

450

5.1.5 LAD of Areosphaeridium diktyoplokum

- Core position: U1411C-8H-4A, 150.11 m CCSF-A.
- 454 *Magnetostratigraphic calibration:* 9 % of Chron C13n.
- 455 Position with regard to calcareous nannoplankton zonation: NP21.
- 456 Age assignment: 33.7 Ma.
 - Discussion: In our material from IODP Expedition 342, the LAD of Areosphaeridium diktyoplokum post-dates the Eocene/Oligocene boundary by 0.2 Ma. Highly similar LADs are suggested from other sites in the North Atlantic. In the Norwegian-Greenland Sea, A. diktyoplokum disappears within Chron C13 between 33.3 and 33.5 Ma (Eldrett et al., 2004). In the Labrador Sea, its LAD falls within NP21/NP22 (Head and Norris, 1989). In the North Sea Basin, the taxon disappears in the lowermost part of Chron C12r (Śliwińska et al., 2012), which is consistent with the indirect calibration of this bioevent against NP21/NP22 in that region (Bujak and Mudge, 1994; Van Simaeys et al., 2005a). While the LADs of A. diktyoplokum as registered in the greater North Atlantic region are highly consistent, the available information suggests a slightly later disappearance in the Tethyan realm. In Italy, A. diktyoplokum has been reported to occur consistently in lowermost Oligocene strata, and its LAD has been calibrated against a level close to the top of Chron C13n at 33.4 Ma (Pross et al., 2010; compare also discussion in Brinkhuis and Visscher, 1995, and van Mourik and Brinkhuis, 2005, and references therein). On the basis of the temporal resolution of the available sample sets, the diachroneity between the North Atlantic and Tethyan LADs of *A. diktyoplokum* amounts to ~0.4 Myr.

474 475 5.1.6 LAD of Charlesdowniea clathrata 476 Core position: U1411C-8H-4A, 150.11 m CCSF-A. 477 Magnetostratigraphic calibration: 9 % of Chron C13n. 478 Position with regard to calcareous nannoplankton zonation: NP21. 479 Age assignment: 33.7 Ma. 480 Discussion: Charlesdowniea clathrata is relatively rare in the studied material; it has 481 not been reported previously from the western North Atlantic. In the eastern North 482 Sea Basin, the species has a mid-Rupelian LAD (Schiøler, 2005). In the western 483 Tethys, the magnetostratigraphically-calibrated LAD of *C. clathrata* was determined 484 as 32.4 Ma (Pross et al., 2010). These findings suggest a pronounced diachroneity 485 between the LADs of C. clathrata in the Tethyan realm and the North Atlantic, which 486 amounts to ~1.3 Myr based on the temporal resolution of the available data. 487 488 5.1.7 FAD of Filisphaera filifera 489 Core position: U1411C-8H-4A, 150.11 m CCSF-A. 490 Magnetostratigraphic calibration: 9 % of Chron C13n. 491 Position with regard to calcareous nannoplankton zonation: NP21. 492 Age assignment: 33.7 Ma. 493 Discussion: In the IODP Expedition 342 material, Filisphaera filifera occurs 494 repeatedly (albeit in low numbers) in the upper Eocene and lowermost Oligocene; 495 the taxon then reappears in the upper Rupelian (corresponding to an age of 29.3 496 Ma). As F. filifera has originally been described from the Neogene and Quaternary 497 (Head, 1994), our findings imply a greatly extended range of this taxon in comparison 498 to previous work. However, they are broadly consistent with previous observations 499 from the North Sea Basin, where F. filifera has been reported from late Oligocene 500 and early Miocene strata (D. Zevenboom, cited in Head, 1994; Van Simaeys et al., 501 2005a).

502 503 5.1.8 FAD of Spiniferites manumii 504 Core position: U1411C-8H-4A, 150.11 m CCSF-A. 505 Magnetostratigraphic calibration: 9 % of Chron C13n. 506 Position with regard to calcareous nannoplankton zonation: NP21. 507 Age assignment: 33.7 Ma. 508 Discussion: Spiniferites manumii occurs persistently, albeit in low numbers from 33.7 509 Ma onwards in the lower Rupelian of the Newfoundland Drift sediments studied. In 510 the Norwegian Sea, the FAD of S. manumii is calibrated to 31.4 Ma for ODP Site 985 511 based on the export of magnetostratigraphical signals from ODP Site 643 (Williams 512 and Manum, 1999), and in the Norwegian-Greenland Sea, the taxon appears close 513 to the C13n/C13r reversal (33.0 Ma; Eldrett et al., 2004). Because S. manumii has an 514 extremely short range, the taxon is considered as one of the best intra-Rupelian 515 markers in Europe (Śliwińska et al., 2012; compare also Section 5.1.14). Our new 516 data from the Newfoundland Drift sediments allow us to export this intra-Rupelian 517 marker to the western North Atlantic, where its FAD is only slightly older than in the 518 Norwegian-Greenland Sea. 519 520 5.1.9 LAD of Stoveracysta sp. 1 521 Core position: U1411B-16H-4A, 145.31 m CCSF-A. 522 Magnetostratigraphic calibration: 35 % of Chron C13n. 523 Position with regard to calcareous nannoplankton zonation: NP21. 524 Age assignment: 33.5 Ma. 525 Discussion: Stoveracysta sp. 1 could not be attributed to previously established taxa 526 (compare taxonomic remarks), and the genus Stoveracysta has not been reported 527 previously from the western North Atlantic. Stoveracysta sp. 1 strongly resembles 528 (?) Stoveracysta sp. sensu Biffi and Manum (1988), which has been described from 529 early Miocene sediments of the Marche Region in central Italy (see taxonomic

530 appendix). For the same region, Brinkhuis and Biffi (1993) identified various species 531 of Stoveracysta in the Eocene/Oligocene boundary interval, and Pross et al. (2010) 532 reported a magnetostratigraphically-calibrated LAD for representatives of the genus 533 Stoveracysta at 30.9 Ma. These findings postdate our findings from the western 534 North Atlantic. 535 536 5.1.10 FAD of Melitasphaeridium asterium 537 Core position: U1411B-16H-4A, 145.31 m CCSF-A. 538 Magnetostratigraphic calibration: 35 % of Chron C13n. 539 Position with regard to calcareous nannoplankton zonation: NP21. 540 Age assignment: 33.5 Ma. 541 Discussion: To date, the FAD of Melitasphaeridium asterium has not been used as a 542 biostratigraphic datum in the North Atlantic. In the Danish sector of the North Sea 543 Basin, the FAD of *M. asterium* occurs in the lower part of Subchron C16n.1n 544 (Thomsen et al., 2012), which is much earlier than in the western North Atlantic. 545 546 5.1.11 LAD of *Lentinia serrata* complex 547 Core position: U1411B-16H-4A, 145.31 m CCSF-A. 548 Magnetostratigraphic calibration: 69 % of Chron C13n. 549 Position with regard to calcareous nannoplankton zonation: NP21. 550 Age assignment: 33.3 Ma. 551 Discussion: The ornamentation in most of the observed specimens here attributed to 552 the L. serrata complex is reflected in penitabular denticles and parasutural crests as 553 they are characteristic for the genus Lentinia Bujak in Bujak et al. (1980). Our 554 material, however, also contains specimens with a greatly reduced number of 555 denticles, which would allow attribution to the genus Vozzhennikovia Lentin and 556 Williams (1976), and the full range of transitions between both endmembers. As the 557 overall morphological characteristics of the encountered specimens are strongly

reminiscent of *L. serrata*, and even in our excellently preserved material the size and exact shape of the archeopyle (compare discussions in Bujak in Bujak et al., 1980, and Sluijs et al., 2009) is only visible in relatively few specimens, we refer to them as *Lentinia serrata* complex in our study.

In the western North Atlantic, *L. serrata* has been previously observed in the Labrador Sea (Head and Norris, 1989) and off eastern Canada (Fensome et al., 2009). Based on a combination of nannoplankton and well-log data, Fensome et al. (2009) have suggested an earliest Rupelian LAD of this species, which is consistent with our results. In the southern North Sea Basin, *L. serrata* was only observed in the late Eocene (Stover and Hardenbol, 1993), while in the eastern North Sea Basin the species extends into the late Eocene to Rupelian (Heilmann-Clausen and Van Simaeys, 2005a; Śliwińska et al., 2012). In the Tethyan realm, *L. serrata* is known from the uppermost Eocene to lowermost Oligocene of Central Italy (Brinkhuis and Biffi, 1993); it disappears within Chron C12r at 32.4 Ma (Pross et al., 2010). Based on the available sample resolution, the LAD of *L. serrata* in the western Tethys thus postdates the here identified LAD for the *L. serrata* complex in the western North Atlantic by ~0.9 Myr.

5.1.12 FAD of Chiropteridium lobospinosum

- 577 Core position: U1406B-21H-3W, 225.9 m CCSF-A.
- 578 Magnetostratigraphic calibration: 54 % of Chron C12r.
- 579 Position with regard to calcareous nannoplankton zonation: NP22.
- 580 Age assignment: 32.0 Ma.
- Discussion: The FAD of Chiropteridium lobospinosum in the Newfoundland Drift
 sediments postdates its appearance in the Norwegian-Greenland Sea; there, the
 taxon first occurs at 33.5 Ma (Eldrett et al., 2004). In the Labrador Sea, C.
 lobospinosum appears at the beginning of NP23 (Head and Norris, 1989), and for the
 North Sea Basin, the FAD of C. lobospinosum has been indirectly calibrated against

586 NP22 (Köthe, 1990; Van Simaeys et al., 2005a; Śliwińska et al., 2012). In the 587 Tethyan region, Chiropteridium spp. (mainly C. lobospinosum) has already been 588 recorded within the lower part of Chron C12r, and the first consistent occurrence has 589 been calibrated against Subchron C11n.1n at 29.75 Ma (Pross et al., 2010). Hence, 590 C. lobospinosum has a regionally diachronous FAD; in the Norwegian-Greenland 591 Sea, the species appears earlier than in the Newfoundland Drift succession, whereas 592 its FAD in the Tethyan realm it occurs even later than in both these regions. Although 593 not magnetostratigraphically constrained, the FAD in the North Sea sites appears 594 similar to our record. 595 596 4.1.13 FAD of Hystrichokolpoma pusillum 597 Core position: U1406B-21H-3W, 225.9 m CCSF-A. 598 Magnetostratigraphic calibration: 54 % of Chron C12r. 599 Position with regard to calcareous nannoplankton zonation: NP22. 600 Age assignment: 32.0 Ma. 601 Discussion: In the Tethys region, the FAD of Hystrichokolpoma pusillum is dated at 602 32.3 Ma (Pross et al., 2010) and thus (considering our sampling resolution of ~150 603 kyrs) is virtually synchronous with the appearance of the species in the western 604 North Atlantic. 605 606 5.1.14 LAD of Spiniferites manumii 607 Core position: U1406C-21X-4W, 222.24 m CCSF-A. 608 Magnetostratigraphic calibration: 73 % of Chron C12r. 609 Position with regard to calcareous nannoplankton zonation: NP22. 610 Age assignment: 31.6 Ma. 611 Discussion: In the Norwegian-Greenland Sea, the LAD of Spiniferites manumii is 612 observed in the upper part of Chron C12r at ~30.8 Ma (Eldrett et al. 2004; recorded 613 as Spiniferites sp. 1 sensu Manum et al. 1989). In the North Sea Basin, the LAD of

614 the species is indirectly calibrated against the upper part of Chron C12r (Lagrou et 615 al., 2004; Van Simaeys et al., 2005a), and biostratigraphically calibrated against the 616 upper part of NP23 (Van Simaeys et al., 2005a). We conclude that the FAD 617 (compare Section 5.1.9) and LAD of S. manumii are thus remarkably synchronous 618 across the greater North Atlantic region. The highly restricted stratigraphic range of 619 ~2 Ma makes S. manumii an exceptionally good intra-Rupelian marker for this 620 region. 621 622 5.1.15 LAD of *Phthanoperidinium comatum* 623 Core position: U1406B-20H-1W, 209.15 m CCSF-A. 624 *Magnetostratigraphic calibration:* 75 % of Chron C12n. 625 Position with regard to calcareous nannoplankton zonation: NP23. 626 Age assignment: 30.7 Ma. 627 Discussion: The LAD of Phthanoperidinium comatum as derived from our dataset 628 agrees with the record of Head and Norris (1989) from the Labrador Sea, where the 629 LAD is calibrated against NP23. This is consistent with the early Rupelian LAD of P. 630 comatum in the Danish North Sea (Schiøler, 2005). For the western Tethys, Pross et 631 al. (2010) reported rare findings of *P. comatum* until the end of Chron C9r. Hence, 632 our results show an apparently synchronous LAD of the species in our dataset and 633 other North Atlantic sites, but a diachroneity between these North Atlantic sites and 634 the Tethyan region, where the species disappears later. 635 636 5.1.16 FAD of Chiropteridium galea 637 Core position: U1406A-19H-5W, 204.73 m CCSF-A. 638 Magnetostratigraphic calibration: 31 % of Chron C11r. 639 Position with regard to calcareous nannoplankton zonation: NP23. Age assignment: 30.5 Ma. 640

Discussion: The FAD of Chiropteridium galea is a well-known biostratigraphic datum for the latest Eocene to earliest Oligocene (Williams and Bujak, 1985; Damassa et al., 1990). Its FAD in the Norwegian-Greenland Sea is between 33.5 and 33.1 Ma (Eldrett et al., 2004). For the Labrador Sea, where it occurs much earlier, a biostratigraphically calibrated FAD of the species has been determined at the beginning of NP18 (as Chiropteridium mespilanum; Head and Norris, 1989). Data from the southern North Sea Basin indicate an indirectly calibrated FAD of Chiropteridium spp. in the uppermost part of NP22 (Van Simaeys et al., 2005a); the FAD of C. galea (i.e., a member of the Chiropteridium plexus) in northwestern Germany occurs at the same time (Köthe, 1990). A comparison of available FADs within the North Atlantic region suggests a strong diachroneity, with the earliest FAD in the Labrador Sea (NP18, i.e., older than 38.1 Ma; Head and Norris, 1989) and a much later FAD (30.5 Ma - this study) off Newfoundland. The FAD of C. galea within the Norwegian-Greenland Sea (Eldrett et al., 2004) also predates the FAD as identified in the Newfoundland Drift succession, whereas data from the North Sea Basin (Van Simaeys et al., 2005a; Köthe, 1990; at least 32.9 Ma) suggest a later first appearance in that region.

658

659

657

641

642

643

644

645

646

647

648

649

650

651

652

653

654

655

656

5.1.17 FAD of Oligokolpoma galeottii

- 660 *Core position:* U1406A-19H-5W, 204.73 m CCSF-A.
- 661 Magnetostratigraphic calibration: 31 % of Chron C11r.
- Position with regard to calcareous nannoplankton zonation: NP23.
- Age assignment: 30.4 Ma.
- Discussion: Oligokolpoma galeottii Pross et al., 2010 has previously been described
- from the western Tethys (Pross et al., 2010) with an FAD in the uppermost part of
- 666 Chron C12r, at 31.3 Ma. In our records from the Newfoundland Drift sediments, the
- taxon appears slightly later, at 30.4 Ma.

668

669	5.1.18 FAD of Artemisiocysta cladodichotoma
670	Core position: U1411B-10H-2W, 81.6 m CCSF-A.
671	Magnetostratigraphic calibration: not identified, between Subchrons C11n.2n and
672	C10n.2n.
673	Position with regard to calcareous nannoplankton zonation: NP23/NP24.
674	Age assignment: 29.6 Ma-28.3 Ma (based on a linear interpolation).
675	Discussion: In our Newfoundland Drift material, specimens of Artemisiocysta
676	cladodichotoma were identified in three samples from a short interval in Hole
677	U1411B without reliable magnetostratigraphic information. Based on linear
678	interpolation, the age can be constrained to fall between 29.6 Ma and 28.3 Ma. In
679	younger strata, A. cladodichotoma is continuously present from 22.7 Ma onwards. In
680	the North Sea Basin, the FAD of A. cladodichotoma is considered an important
681	biostratigraphic marker for the basal Chattian (Van Simaeys et al. 2005a). In
682	successions from the Danish sector of the North Sea Basin, the taxon is extremely
683	rare and only occurs across a short interval straddling the magnetochron C9r/C9n
684	reversal (Śliwińska et al., 2012). In the Umbria-Marche Basin of Central Italy, A.
685	cladodichotoma is already observed in Chrons C8 and C9n (Pross et al., 2010).
686	Despite the remaining uncertainties in our age assignment from Site U1411, a
687	considerably earlier FAD of A. cladodichotoma emerges for the western North
688	Atlantic. This offset may well be due to paleoceanographic factors, its inconspicuous
689	appearance (easily overlooked) and/or the rarity of the taxon in Chattian dinocyst
690	assemblages.
691	
692	5.1.19 LAD of Enneadocysta pectiniformis
693	Core position: U1406B-17H-2W, 165.59 m CCSF-A.
694	Magnetostratigraphic calibration: Chron C9n.
695	Position with regard to calcareous nannoplankton zonation: NP25.
696	Age assignment: 26.7 Ma.

Discussion: Enneadocysta pectiniformis (Gerlach, 1961) Stover and Williams, 1995 differs from Enneadocysta arcuata (Eaton, 1971) Stover and Williams, 1995 through the absence of plate 6'' and thus also the process on plate 6''; however, the plate is not a necessarily present feature for *E. arcuata* (Stover and Williams, 1995, Table 2). As this difference is not always observable, and their overall morphologies and sizes are highly similar, the two species were not separated in the present study and counted as *E. pectiniformis* following Schiøler (2005).

In the Labrador Sea, the LADs of *E. arcuatum* and *E. pectiniformis* are calibrated against NP23 and NP 24, respectively (Head and Norris, 1989). For the North Sea Basin, Van Simaeys et al. (2005a) report *E. pectiniformis* to disappear in the middle part of NP23, while Schiøler (2005) decribes an LAD of *Enneadocysta* spp. within the upper half of the Rupelian. For the western Tethys, Pross et al. (2010) reported a LAD of *E. pectiniformis* at 27.9 Ma. We conclude that the LAD of *E. pectiniformis* in the Newfoundland Drift sediments postdates the LADs available for the Labrador Sea, North Sea Basin and Tethyan region. The apparent discrepancy in LADs between the Tethys and the North Sea Basin has been previously observed by Pross et al. (2010), who connected it to a gradual abundance decline of *E. pectiniformis* towards its range top.

5.1.20 LAD of Areoligera semicirculata

- *Core position:* U1406C-16H-5W, 155.89 m CCSF-A.
- *Magnetostratigraphic calibration:* 27 % of Chron C8r.
- 719 Position with regard to calcareous nannoplankton zonation: NP25.
- 720 Age assignment: 26.3 Ma.
- 721 Discussion: Areoligera semicirculata is rather rare in the material from the
- Newfoundland Drift and never reaches more than 1% of the dinocyst assemblages.
- 723 In the Norwegian Sea, the LAD of *A. semicirculata* has been
- magnetostratigraphically calibrated at 30.4 Ma (Williams and Manum, 1999). Its LAD

is an important marker for the early Chattian in NW Europe (Köthe, 1990; Van Simaeys et al., 2005a). In Denmark, *A. semicirculata* is common within Chron C8r (Śliwińska et al. 2012). In the western Tethys, the LAD occurs within Chron C9n at 27.4 Ma (Pross et al. 2010). Hence, the LAD for the Newfoundland Drift succession is in close agreement with the data from the North Sea. Diachroneities exist for the Labrador Sea and the Tethys, where *A. semicirculata* disappears earlier.

5.1.21 LAD of Saturnodinium pansum

- *Core position:* U1406C-16H-5W, 155.89 m CCSF-A.
- 734 Magnetostratigraphic calibration: 27 % of Chron C8r.
- 735 Position with regard to calcareous nannoplankton zonation: NP25.
- 736 Age assignment: 26.3 Ma.
 - Discussion: Saturnodinium pansum was first described from middle to upper

 Oligocene strata of the Blake Plateau, North Atlantic (Stover, 1977). To date, there is no record of *S. pansum* in the Norwegian Sea, although other Chattian taxa such as Areoligera semicirculata or Distatodinium biffii are present there (KKS, unpublished data). In contrast, *S. pansum* is well known from the North Sea Basin. There, its LAD is biostratigraphically calibrated against the basal part of the alternative NP25* (for details see Van Simaeys et al. 2005a). In the German sector of the North Sea Basin, the taxon was observed within the Aquitanian (Köthe and Piesker, 2007), while in the eastern North Sea Basin the taxon was never observed above the mid-Chattian (i.e., Chron C8r; Śliwińska et al., 2012; K. Dybkjær, personal communication). In the Mediterranean region, the taxon was reported from the lower Rupelian (Chron C12r) and upper Chattian (Chron C7n- C6?; Pross et al., 2010). Summarizing the available evidence, we observe a synchronous dissaperance of *S. pansum* in the Newfoundland Drift region and the eastern North Sea Basin. Notably, these regions have also yielded the northernmost records of *S. pansum* as yet known. The

752	observed distribution pattern of S. pansum may furthermore suggest that the taxon is
753	adapted to relatively warm surface waters.
754	
755	5.1.22 LAD of Wetzeliella gochtii/symmetrica group
756	Core position: U1406B-14H-5W, 144.73 m CCSF-A.
757	Magnetostratigraphic calibration: 13 % of Subchron C8n.2n.
758	Position with regard to calcareous nannoplankton zonation: NP25.
759	Age assignment: 25.9 Ma.
760	Discussion: In the Newfoundland Drift sediments, Wetzeliella spp. mainly comprise
761	W. gochtii and W. symmetrica as well as transitional forms between these two taxa.
762	At the Scotian Margin off Canada, W. gochtii exhibits a middle Chattian LAD, and the
763	LAD of W. symmetrica is at the top of the Chattian (Fensome et al., 2009). In the
764	Labrador Sea, W. symmetrica occurs until NP24 (Head and Norris, 1989). In the
765	North Sea, the LAD of W. symmetrica has been determined at the NP24/NP25
766	boundary, and the LAD of W. gochtii has been recorded within the lowermost NP25
767	(Van Simaeys et al., 2005a). This North Sea datum also applies to Schiøler (2005),
768	who provides a LAD for the W. gochtii/W. symmetrica group in the basal Chattian. In
769	the western Tethys, only W. gochtii was found, which has a LAD at 26.9 Ma (Pross et
770	al., 2010). In the Labrador Sea and the North Sea Basin, species of the genus
771	Wetzeliella disappear earlier than in the Newfoundland Drift succession.
772	
773	5.1.23 LAD of Filisphaera filifera
774	Core position: U1405A-15H-3W, 173.86 m CCSF-A.
775	Magnetostratigraphic calibration: 25 % of Subchron C6Cn.2n.
776	Position with regard to calcareous nannoplankton zonation: NN1.
777	Age assignment: 22.7 Ma.
778	Discussion: Filisphaera filifera has not been reported from the North Atlantic before.
779	In the North Sea Basin, the taxon disappears at the Oligocene-Miocene boundary

780 (Schiøler, 2005), which is very close to the LAD identified for the Newfoundland Drift 781 successions. However, F. filifera also occurs in the younger Neogene and 782 Quaternary (Head, 1994; compare Section 5.1.8). 783 784 5.1.24 LAD of Hystrichokolpoma pusillum 785 Core position: U1405A-16H-4W, 185.92 m CCSF-A. 786 Magnetostratigraphic calibration: 69 % of Subchron C6Cn.1r. 787 Position with regard to calcareous nannoplankton zonation: NN2. 788 Age assignment: 22.8 Ma. 789 Discussion: Based on the available information, Hystrichokolpoma pusillum exhibits 790 strongly diachronous range tops in the western North Atlantic (this study), the North 791 Sea (Schiøler, 2005) and the western Tethys (Biffi and Manum, 1988). In the North 792 Sea, H. pusillum disappears in the uppermost Rupelian (Schiøler, 2005). In the 793 western Tethys, the taxon occurs regularly until at least 23.6 Ma (Pross et al., 2010); 794 its LAD is during NN1 (Biffi and Manum, 1988). Thus, the even younger LAD 795 registered for the Newfoundland Drift material may mark the youngest occurrence of 796 H. pusillum as yet known. 797 798 799 5.1.25 LAD of Deflandrea spp. 800 Core position: U1405A-14H-5W, 167.71 m CCSF-A. 801 Magnetostratigraphic calibration: 25 % of Subchron C6Bn.2n. 802 Position with regard to calcareous nannoplankton zonation: NN2. 803 Age assignment: 22.2 Ma. 804 Discussion: The LAD of Deflandrea spp., mostly represented by the species D. 805 phosphoritica, is a classical biostratigraphic marker for the Oligocene-Miocene 806 boundary interval. For the Scotian Margin off Canada, Fensome et al. (2009) 807 reported the LAD of *Deflandrea* spp. to coincide with the top of the Chattian, which is consistent with our findings from the Newfoundland Drift succession. Data on the LAD of *Deflandrea* spp. in the North Sea Basin suggest a more complex disappearance pattern for that region. In the Danish sector of the North Sea Basin, Dybkjær et al. (2012) used *D. phosphoritica* in their characterization of the Oligocene-Miocene boundary. They observed *D. phosphoritica* in the late Chattian and early Aguitanian, with the taxon disappearing shortly before the Oligocene-Miocene boundary and then repeatedly re-occuring in the basal Aguitanian. Findings of *Deflandrea* spp. in the lower Miocene of the same region have previously been reported by Schiøler (2005). 5.1.26 FAD and LAD of Svalbardella spp.

817

818

819

824

825

826

827

828

829

830

831

832

833

834

808

809

810

811

812

813

814

815

816

- Core position: for the FAD U1411C-8H-4A, 150.11 m CCSF-A; for the LAD U1405B-
- 820 15H-5W, 160.95 m CCSF-A.
- 821 Magnetostratigraphic calibration: 8 % of Chron C13n to 61 % of Subchron C6Bn.2n.
- 822 Position with regard to calcareous nannoplankton zonation: NP21-NN2.
- 823 Age assignment: 33.7-22.1 Ma.
 - Discussion: Svalbardella spp. reaches exceptionally high abundances and exhibits repeated recurrences in the Newfoundland Drift material. The genus Svalbardella is a typical representative of high-latitude North Atlantic dinocyst assemblages during the middle to late Eocene and the Oligocene (Manum 1960, 1976; Manum and Throndsen, 1986; Head and Norris, 1989; Eldrett et al., 2004). During surface-water cooling pulses associated with Oligocene glacial episodes, the genus also briefly occurred in the North Sea (Van Simaeys, 2004; Śliwińska et al., 2010; Śliwińska and Heilmann-Clausen, 2011; Clausen et al., 2012), the Tethyan realm (Brinkhuis and Biffi, 1993; Van Simaeys et al., 2005b; Coccioni et al., 2008; Pross et al., 2010), and the high latitudes of the southern hemisphere (Brinkhuis et al., 2003; Van Simaeys et al., 2005b). As such, the genus represents arguably the best indicator of surface-

water cooling in Paleogene dinocyst assemblages (compare Sluijs et al., 2005) and thus has attracted considerable attention over the past 15 years or so.

835

836

837

838

839

840

841

842

843

844

845

846

847

848

849

850

851

852

853

854

855

856

857

858

859

860

861

862

The two most important features that distinguish the genus Svalbardella from the morphologically similar genus Palaeocystodinium are a visible paracingulum and bluntly rounded apical and antapical horns. To date, the genus comprises two formally established species, S. cooksoniae (Manum, 1960) and S. partimtabulata (Heilmann-Clausen and Van Simaeys, 2005). However, in addition to these species, a number of similar dinocyst morphotypes has informally and peripherally been referred to Svalbardella (e.g., Schiøler, 2005; Śliwińska et al., 2012). Some of these morphotypes exhibit clearly rounded horns, but lack a visible paracingulum and are therefore sometimes referred to as *Palaeocystodinium* (e.g., Damassa et al., 1996). This morphological variety of the Svalbardella/Palaeocystodinium complex is also documented in our material from the Newfoundland Drift succession (Plate VII, 12-15). To avoid nomenclatoric confusion, we have attributed 'Svalbardella/Palaeocystodinium-like' dinocyst morphotypes to Svalbardella spp. if they exhibited rounded horns and/or paracingular tabulation. It has been speculated that the morphology may have been affected by sea-surface temperature (e.g., Van Simaeys et al., 2005b). In the Norwegian Sea, S. cooksoniae appears at 42.2 Ma (Eldrett et al., 2004). In the eastern North Sea Basin, S. partimtabulata appears first in Chron C18r and the upper part of NP16 (Heilmann-Clausen and Van Simaeys, 2005; Thomsen et al., 2012). Hence, the oldest documentation of Svalbardella spp. in our Newfoundland Drift material may not necessarily represent the true FAD of Svalbardella spp. in the western North Atlantic. In the Labrador Sea, the LAD of S. cooksoniae is indirectly calibrated to NP23 (Head and Norris, 1989). Significantly earlier LADs have been reported from the Norwegian Sea (30.4 Ma, ODP Site 985; Williams and Manum, 1999) and the Norwegian-Greenland Sea (33.5 Ma, ODP Sites

338 and 643A; Eldrett et al., 2004). In the North Sea Basin, the youngest records of

Svalbardella spp. are from the lower Chattian (Schiøler, 2005) and Chron C9n (Śliwińska et al., 2012), respectively. In the western Tethys, Coccioni et al. (2008) and Pross et al. (2010) recorded a recurrence interval of *Svalbardella* spp. between 29.1 and 27.1 Ma; it coincides with the Oi-2b benthic δ^{18} O glacial episode of Miller et al. (1991), which represents the strongest glaciation of the Oligocene (Pälike et al., 2006). Summarizing the above, the occurrence pattern of *Svalbardella* spp. is strongly controlled by the regionally prevailing surface-water temperature regime. In light of the high variability of Oligocene climates, their FADs and LADs can hence only be employed for short-distance correlations on intra-basinal scales. On the other hand, *Svalbardella* spp. can serve as a highly sensitive paleoenvironmental indicator for changes in surface-water temperatures.

5.2 Additional observations

Although the Newfoundland Drift sediments have yielded highly diverse dinocyst assemblages, a number of well-known biostratigraphic markers for the Oligocene of the North Atlantic region are poorly represented or even conspicuously absent. For instance, only single specimens of *Distatodinium biffii* and *Rhombodinium draco* were encountered in the study material. *Distatodinium biffii* is an important marker for the Rupelian-Chattian boundary in the North Sea (Śliwińska et al., 2012) and in the Tethyan realm (Coccioni et al., 2008; Pross et al., 2010). The same holds for *R. draco*, the LAD of which biostratigraphically defines the Rupelian-Chattian boundary and the lowermost part of the Chattian in the North Sea (Köthe, 1990; Schiøler, 2005; Van Simaeys et al., 2005a).

The Eocene-Oligocene transition interval of the Newfoundland Drift succession is characterized by a number of LADs of typical lower-latitude, Tethyan marker species such as *Schematophora speciosa*, *Hemiplacophora semilunifera*, and *Cordosphaeridium* cf. *funiculatum* (Fig. 5). Considering that cyst-forming dinoflagellates are highly sensitive to changes in the shallow surface waters,

especially with regard to changes in temperature (e.g., Sluijs et al., 2005), the disappearance of these lower-latitude taxa during the latest Eocene and earliest Oligocene points to surface-water cooling off Newfoundland, possibly due to an enhanced influence of the proto-Labrador Current.

This hypothesis is supported by the first documentation of the cold-water indicator *Svalbardella* spp. in the same interval, which also suggests a surface-water cooling. This can be explained by the southward expansion of cool surface-water masses from the high northern latitudes where surface-water temperatures declined earlier. In the Labrador Sea, the genus *Svalbardella* already appears during the early Eocene (Head and Norris, 1989).

6 Concluding remarks

Our detailed dinocyst study on the Newfoundland Drift sediments recovered during IODP Expedition 342 has yielded the first magnetostratigraphically-calibrated dinocyst bioevents for the uppermost Eocene to lowermost Miocene of the western North Atlantic. Comparison with magnetostratigraphically-calibrated dinocyst datums from elsewhere in the North Atlantic, the North Sea, and the western Tethys helps to quantify spatial leads and lags for a number of dinocyst events, although such efforts are hindered by the yet low availability of chronostratigraphically constrained appearance data from many regions. For the Eocene-Oligocene boundary interval, we observe a high degree of synchronicity between dinocysts bioevents offshore Newfoundland and in the western Tethys (e.g., Schematophora speciosa, Cordosphaeridium cf. funiculatum and Hemiplacophora semilunifera).

The demise of lower-latitude taxa across the Eocene-Oligocene transition interval in concert with the appearance of the cold-water indicator *Svalbardella* spp. points to a surface-water cooling off Newfoundland during that time. Due to the applicability of dinocyst biostratigraphy to high-latitude settings, and considering that calcareous and siliceous plankton groups exhibit reduced diversities, relatively low

preservation potential or both in polar to sub-polar environments, the dinocyst bioevents identified and independently dated in our study contribute to an improved age framework for future paleoceanographical studies in the higher-latitude North Atlantic. Ultimately, the chronostratigraphically constrained dinocyst bioevents identified in our study may contribute to an improved understanding of the paleoclimatic and paleoceanographic evolution of the Oligocene world.

Acknowledgments

This research used samples and data provided by the Integrated Ocean Drilling Program, which was sponsored by the US. National Science Foundation and participating countries under management of Joint Oceanographic Institutions Inc. Invaluable support of the members of the IODP Expedition 342 Science Party is gratefully acknowledged. André Bahr and Martin Head are thanked for discussions, and Malcolm Jones is thanked for technical support. Financial support through the German Research Foundation (DFG; grants PR651/16-3 and FR2544/8 to J.P. and O.F., respectively) and the Danish Council for Independent Research/Natural Sciences (DFF/FNU; grant 11-107497 to K.K.Ś.) is gratefully acknowledged.

Appendix A. Taxonomic remarks

An alphabetical list of all identified dinocyst taxa is given in Table A.1, and selected taxa are depicted on Plates I–VIII. For taxonomic citations, we refer to Fensome and Williams (2004) and the updated online version (Fensome et al., 2008); only taxa and emendations that are not included into these reference catalogues are treated here.

Selected taxonomy

- 945 Division: DINOFLAGELLATA (Bütschli, 1885) Fensome et al., 1993
- 946 Subdivision: DINOKARYOTA Fensome et al., 1993

947	Class: DINOPHYCEAE Pascher, 1914
948	Subclass: PERIDINIPHYCIDEAE Fensome et al., 1993
949	Order: GONYAULACALES Taylor, 1980
950	Suborder: GONYAULACINEAE Fensome et al., 1993
951	Family: GONYAULACINEAE Lindemann, 1928
952	Subfamily: GONYAULACINEAE Fensome et al., 1993
953	
954	Genus: STOVERACYSTA Clowes, 1985
955	Stoveracysta sp. 1
956	Pl. VII, 10, 11
957	Dimensions: mean width: 41.2 μm, mean archeopyle diameter: 30.5 μm, mean
958	overall length: 54 μm (n=5).
959	Description: Stoveracysta sp. 1 is a morphotype of Stoveracysta with one apical and
960	two antapical protrusions that are not always expressed. The ornamentation of the
961	ectophragm consists of low (c. 2 µm high), perforate penitabular septa, and plate 1
962	is very small.
963	Remarks: The species resembles (?) Stoveracysta sp. of Biffi and Manum (1988, p.
964	194-196, Pl. 7, Figs. 10-11 and 13-14) in having two antapical lobes and an
965	ectophragm that forms penitabular ridges. However, Stoveracysta sp. 1 differs from
966	(?) Stoveracysta sp. of Biffi and Manum (1988) in lacking a visible cingulum, but
967	showing other clearly visible plates. Furthermore, (?) Stoveracysta sp. of Biffi and
968	Manum (1988) has continuous rather than perforate septa/membranes.
969	
970	
971	Literature
972	Backman, J., 1987. Quantitative calcareous nannofossil biochronology of middle
973	Eocene through early Oligocene sediments from DSDP sites 522 and 523.
974	Abhandlungen der Geologischen Bundesanstalt 39, 21-31

975	Baldauf, J., Barron, J., 1990. Evolution of Biosiliceous Sedimentation Patterns —
976	Eocene through Quaternary: Paleoceanographic Response to Polar Cooling.
977	In: Bleil, U., Thiede, J. (Eds.), Geological History of the Polar Oceans: Arctic
978	versus Antarctic. Springer, Netherlands, 575-607.
979	Beaudoin, A.B., Head, M.J., 2004. The Palynology and Micropalaeontology of
980	Boundaries. Geological Society of London, Special Publication 230, London.
981	Biffi, U., Manum, S.B., 1988. Late Eocene–Early Miocene dinoflagellate cyst
982	stratigraphy from the Marche Region (central Italy). Bollettino della Società
983	Paleontologica Italiana 27, 163-212.
984	Boersma, A., Silva, I.P., 1991. Distribution of Paleogene planktonic foraminifera —
985	analogies with the recent?. Palaeogeography, Palaeoclimatology,
986	Palaeoecology 83, 29-47.
987	Brinkhuis, H., Biffi, U., 1993. Dinoflagellate cyst stratigraphy of the
988	Eocene/Oligocene transition in central Italy. Marine Micropaleontology 22,
989	131-183.
990	Brinkhuis, H., Munsterman, D.K., Sengers, S., Sluijs, A., Warnaar, J., Williams, G.L.,
991	2003. Late Eocene-Quaternary Dinoflagellate Cysts from ODP Site 1168, off
992	Western Tasmania. In: Exon, N.F., Kennett, J.P., Malone, M.J. (Eds.),
993	Proceedings of the Ocean Drilling Program, Scientific Results, pp. 1-36.
994	Bujak, J., Mudge, D., 1994. A high-resolution North Sea Eccene dinocyst zonation.
995	Journal of the Geological Society 151, 449-462.
996	Bukry, D., 1973. Low-Latitude Coccolith Biostratigraphic Zonation. In: Larson, R,L.,
997	Moberly, R. (Eds.), Initial Reports of the Deep Sea Drilling Project Vol. 15, pp.
998	685-703.
999	Clausen, O.R., Śliwińska, K.K., Gołędowski, B., 2012. Oligocene climate changes
1000	controlling forced regression in the eastern North Sea. Marine and Petroleum
1001	Geology 29, 1-14.

1002 Coccioni, R., Marsili, A., Montanari, A., Bellanca, A., Neri, R., Bice, D.M., Brinkhuis, 1003 H., Church, N., Macalady, A., McDaniel, A., Deino, A., Lirer, F., Sprovieri, M., 1004 Maiorano, P., Monechi, S., Nini, C., Nocchi, M., Pross, J., Rochette, P., 1005 Sagnotti, L., Tateo, F., Touchard, Y., Van Simaeys, S., Williams, G., 2008. 1006 Integrated stratigraphy of the Oligocene pelagic sequence in the Umbria-1007 Marche basin (northeastern Apennines, Italy): a potential global stratotype 1008 section and point (GSSP) for the Rupelian/Chattian boundary. Geological 1009 Society of America Bulletin 120, 487-511. 1010 Coxall, H.K., Wilson, P.A., Pälike, H., Lear, C.H., Backman, J., 2005. Rapid stepwise 1011 onset of Antarctic glaciation and deeper calcite compensation in the Pacific 1012 Ocean. Nature 433, 53-57. 1013 Damassa, S.P., Goodman, D.K., Kidson, E.J., Williams, G.L., 1990. Correlation of 1014 Paleogene dinoflagellate assemblages to standard nannofossil zonation in 1015 North Atlantic DSDP sites. Review of Palaeobotany and Palynology 65, 331-1016 339. 1017 Davies, R., Cartwright, J., Pike, J., Line, C., 2001. Early Oligocene initiation of North 1018 Atlantic deep water formation. Nature 410, 917-920. 1019 Dybkjær, K., King, C., Sheldon, E., 2012. Identification and characterisation of the 1020 Oligocene-Miocene boundary (base Neogene) in the eastern North Sea 1021 basin based on dinocyst stratigraphy, micropalaeontology and δ^{13} C-1022 isotope data. Palaeogeography, Palaeoclimatology, Palaeoecology 363, 11-1023 22. 1024 Eldrett, J.S., Harding, I.C., 2009. Palynological analyses of Eocene to Oligocene 1025 sediments from DSDP site 338, outer Vøring plateau. Marine 1026 Micropaleontology 73, 226-240. 1027 Eldrett, J.S., Harding, I.C., Firth, J.V., Roberts, A.P., 2004. Magnetostratigraphic 1028 calibration of Eocene–Oligocene dinoflagellate cyst biostratigraphy from the 1029 Norwegian-Greenland Sea. Marine Geology 204, 91-127.

1030	Fensome, R.A., Williams, G.L., 2004. The Lentin and Williams Index of fossil
1031	dinoflagellates 2004 Edition. American Association of Stratigraphic
1032	Palynologists, Contributions Series Vol. 42, 909 p.
1033	Fensome, R.A., Guerstein, R., Williams, G.L., 2006. New insights on the Paleogene
1034	dinoflagellate cyst genera Enneadocysta and Licracysta gen. Nov. based on
1035	material from offshore eastern Canada and southern Argentina.
1036	Micropaleontology 52, 385-410.
1037	Fensome, R.A., Williams, G.L., MacRae, R.A., 2009. Late Cretaceous and Cenozoic
1038	fossil dinoflagellates and other palynomorphs from the Scotian Margin,
1039	offshore eastern Canada. Journal of Systematic Palaeontology 7, 1-79.
1040	Firth, J., Eldrett, J., Harding, I., Coxall, H., Wade, B., 2012. Integrated
1041	Biomagnetochronology for the Palaeogene of ODP Hole 647A: Implications
1042	for Correlating Palaeoceanographic Events from High to Low Latitudes. In:
1043	Jovane, L., Herrero-Bervera, E., Hinnov, L.A., Housen, B.A. (Eds.), Magnetic
1044	Methods and the Timing of Geological Processes. Geological Society of
1045	London, Special Publications Vol. 373, SP373-SP379.
1046	Gradstein, F.M., Ogg, J.G., Schmitz, M., Ogg, G., 2012. The Geologic Time
1047	Scale 2012. Elsevier, Amsterdam.
1048	Head, M.J., 1994. Morphology and paleoenvironmental significance of the Cenozoic
1049	dinoflagellate genera Tectatodinium and Habibacysta. Micropaleontology 40,
1050	289-321.
1051	Head, M.J., Norris, G., 1989. 28. Palynology and Dinocyst Stratigraphy of the
1052	Eocene and Oligocene in ODP Leg 105, Hole 647A, Labrador Sea. In:
1053	Strivastava, S.P., Arthur, M., Clement, B., et al. (Eds.), Ocean Drilling
1054	Program, Proceedings, Scienfific Results, Vol. 105, pp. 423-451.
1055	Heilmann-Clausen, C., Van Simaeys, S., 2005. Dinoflagellate cysts from the middle
1056	Eocene to ?Lowermost Oligocene succession in the Kysing research
1057	borehole, central Danish basin. Palynology 29, 143-204.

1058 Houben, A.J., Bijl, P.K., Pross, J., Bohaty, S.M., Passchier, S., Stickley, C.E., Röhl, 1059 U., Sugisaki, S., Tauxe, L., van de Flierdt, T., Olney, M., Sangiorgi, F., Sluijs, 1060 A., Escutia, C., Brinkhuis, H., and the Expedition 318 Scientists, 2013. 1061 Reorganization of Southern Ocean plankton ecosystem at the onset of 1062 Antarctic glaciation. Science 340, 341-344. 1063 Jenkins, J.M., 2013. Applied Micropalaeontology. Springer Science and Business 1064 Media, Luxemburg. 1065 Kempf, O., Pross, J., 2005. The lower marine to lower freshwater Molasse transition 1066 in the northern Alpine foreland basin (Oligocene: Central Switzerland-South 1067 Germany): age and geodynamic implications. International Journal of Earth 1068 Sciences 94, 160-171. 1069 Kender, S., Kaminski, M.A., 2013. Arctic Ocean benthic foraminiferal faunae change 1070 associated with the onset of perennial sea ice in the Middle Miocene. 1071 Journal of Foraminiferal Research 43, 99-109. 1072 Köthe, A., 1990. Paleogene dinoflagellates from Northwest Germany – 1073 biostratigraphy and paleoenvironment. Geologisches Jahrbuch, Reihe A 118, 1074 3-111. 1075 Köthe, A., Piesker, B., 2007. Stratigraphic distribution of Paleogene and Miocene 1076 dinocysts in Germany. Revue de Paléobiologie 26, 1-39. 1077 Kuiper, K., Deino, A., Hilgen, F., Krijgsman, W., Renne, P., Wijbrans, J., 2008. 1078 Synchronizing rock clocks of earth history. Science 320, 500-504. 1079 Lagrou, D., Vandenberghe, N., Van Simaeys, S., Hus, J., 2004. Magnetostratigraphy 1080 and rock magnetism of the Boom Clay (Rupelian stratotype) in Belgium. 1081 Geologie en Mijnbouw/Netherlands Journal of Geosciences 83, 209-225. 1082 Lazarus, D., 1983. Speciation in pelagic Protista and its study in the planktonic 1083 microfossil record: a review. Paleobiology 9, 327-340. 1084 Lipps, J.H., 1993. Fossil Prokaryotes and Protists. Blackwell Scientific 1085 Publications, USA.

1086 Lund, J.J., 2002. A Lower Oligocene Norwegian Sea Dinoflagellate Cyst found in the 1087 North Sea and in the Rupelian type area in Belgium. Northern European 1088 Cenozoic Stratigraphy 83-89. 1089 Luterbacher, H.P., Ali, J.R., Brinkhuis, H., Gradstein, F., Hooker, J., Monechi, S., 1090 Ogg, J., Powell, J., Röhl, U., Sanfilippo, A., 2004. The Paleogene Period. In: 1091 Gradstein, F.M., Ogg, J.G., Smith, A.G. (Eds.), A geologic time scale. 1092 Cambridge University Press, Cambridge, pp. 384-408. 1093 Manum, S., 1976. Dinocysts in Tertiary Norwegian-Greenland Sea sediments (Deep 1094 Sea Drilling Project Leg 38), with observations on palynomorphs and 1095 palynodebris in relation to environment. Initial Reports of the Deep Sea 1096 Drilling Project 38, 897-919. 1097 Manum, S.B., Throndsen, T., 1986. Age of Tertiary formations on Spitsbergen. Polar 1098 Research 4, 103-131. Manum, S.B., Boulter, M.C., Gunnarsdottir, H., Rangnes, K., Scholze, A., 1989. 32. 1099 1100 Eocene to Miocene palynology of the Norwegian Sea (ODP Leg 104). In: 1101 Elholm, Ol. Thiede, J., Taylor, E., et al. (Eds.), Proceedings of the Ocean 1102 Drilling Program, Scientific Results Vol. 104, 611-662. 1103 Martini, E., 1971. Standard Tertiary and Quaternary calcareous nannoplankton 1104 zonation. Proceedings of the Second Planktonic Conference, Roma 1970. 1105 Edition Tecnoscienza, 739-785. 1106 Miller, K.G., Tucholke, B.E., 1983. Development of Cenozoic abyssal circulation 1107 south of the Greenland-Scotland Ridge. In: Bott, M.H.P., Saxov, S., Talwani, 1108 M., Thiede, J. (Eds.), Structure and Development of the Greenland-Scotland 1109 Ridge. Springer US, New York, pp. 549-589. 1110 Miller, K.G., Wright, J.D., Fairbanks, R.G., 1991. Unlocking the ice house: Oligocene-1111 Miocene oxygen isotopes, eustasy, and margin erosion. Journal of 1112 Geophysical Research 96, 6829-6848.

- 1113 Munsterman, D., Brinkhuis, H., 2004. A southern North Sea Miocene dinoflagellate
- 1114 cyst zonation. Netherlands Journal of Geosciences/Geologie en Mijnbouw
- 1115 83, 267-285.
- Nederbragt, A.J., 1992. Paleocology of late Maastrichtian Heterohelicidae (planktic
- foraminifera) from the Atlantic region. Palaeogeography, Palaeoclimatology,
- 1118 Palaeoecology 92, 361-374.
- Norris, R.D., Wilson, P.A., Blum, P., Fehr, A., Agnini, C., Bornemann, A., Boulila, S.,
- Bown, P.R., Cournede, C., Friedrich, O., Ghosh, A.K., Hollis, C.J., Hull, P.M.,
- Jo, K., Junium, C.K., Kaneko, M., Liebrand, D., Lippert, P.C., Liu, Z., Matsui,
- H., Moriya, K., Nishi, H., Opdyke, B.N., Penman, D., Romans, B., Scher,
- H.D., Sexton, P., Takagi, H., Turner, S.K., Whiteside, J.H., Yamaguchi, T.,
- Yamamoto, Y., 2014a. Expedition 342 Summary. In: Norris, R.D., Wilson,
- P.A., Blum, P., and the Expedition 342 Scientists (Eds.), Proceedings of the
- 1126 Integrated Ocean Drilling Program 342, College Station, Texas.
- Norris, R.D., Wilson, P.A., Blum, P., Fehr, A., Agnini, C., Bornemann, A., Boulila, S.,
- Bown, P.R., Cournede, C., Friedrich, O., Ghosh, A.K., Hollis, C.J., Hull, P.M.,
- Jo, K., Junium, C.K., Kaneko, M., Liebrand, D., Lippert, P.C., Liu, Z., Matsui,
- H., Moriya, K., Nishi, H., Opdyke, B.N., Penman, D., Romans, B., Scher,
- H.D., Sexton, P., Takagi, H., Turner, S.K., Whiteside, J.H., Yamaguchi, T.,
- 1132 Yamamoto, Y., 2014b. Site U1405. In: Norris, R.D., Wilson, P.A., Blum, P.,
- and the Expedition 342 Scientists (Eds.). Proceedings of the Integrated
- Ocean Drilling Program 342, College Station, Texas.
- Norris, R.D., Wilson, P.A., Blum, P., Fehr, A., Agnini, C., Bornemann, A., Boulila, S.,
- Bown, P.R., Cournede, C., Friedrich, O., Ghosh, A.K., Hollis, C.J., Hull, P.M.,
- Jo, K., Junium, C.K., Kaneko, M., Liebrand, D., Lippert, P.C., Liu, Z., Matsui,
- 1138 H., Moriya, K., Nishi, H., Opdyke, B.N., Penman, D., Romans, B., Scher,
- H.D., Sexton, P., Takagi, H., Turner, S.K., Whiteside, J.H., Yamaguchi, T.,
- Yamamoto, Y., 2014c. Site U1406. In: Norris, R.D., Wilson, P.A., Blum, P.,

1141 and the Expedition 342 Scientists (Eds.), Proceedings of the Integrated 1142 Ocean Drilling Program 342, College Station, Texas. 1143 Norris, R.D., Wilson, P.A., Blum, P., Fehr, A., Agnini, C., Bornemann, A., Boulila, S., 1144 Bown, P.R., Cournede, C., Friedrich, O., Ghosh, A.K., Hollis, C.J., Hull, P.M., 1145 Jo, K., Junium, C.K., Kaneko, M., Liebrand, D., Lippert, P.C., Liu, Z., Matsui, 1146 H., Moriya, K., Nishi, H., Opdyke, B.N., Penman, D., Romans, B., Scher, H.D., Sexton, P., Takagi, H., Turner, S.K., Whiteside, J.H., Yamaguchi, T., 1147 1148 Yamamoto, Y., 2014d. Site U1411. In: Norris, R.D., Wilson, P.A., Blum, P., 1149 and the Expedition 342 Scientists (Eds.), Proceedings of the Integrated 1150 Ocean Drilling Program 342, College Station, Texas. 1151 Pälike, H., Norris, R.D., Herrle, J.O., Wilson, P.A., Coxall, H.K., Lear, C.H., 1152 Shackleton, N.J., Tripati, A.K., Wade, B.S., 2006. The heartbeat of the 1153 Oligocene climate system. Science 314, 1894-1898. 1154 Peeters, F.J.C., Hoek, R.P., Brinkhuis, H., Wilpshaar, M., De Boer, P.L., 1998. 1155 Differentiating glacio-eustacy and tectonics; a case study involving 1156 dinoflagellate cysts from the Eocene–Oligocene transition of the Pindos 1157 Foreland Basin (NW Greece). Terra Nova 10, 245-249. 1158 Pinet, P.R., Popenoe, P., Nelligan, D.F., 1981. Gulf Stream: reconstruction of 1159 Cenozoic flow patterns over the Blake Plateau. Geology 9, 266-270. 1160 Pross, J., 2001. Dinoflagellate cyst biogeography and biostratigraphy as a tool for 1161 palaeoceanographic reconstructions: an example from the Oligocene of 1162 western and northwestern Europe. Neues Jahrbuch fur Geologie und 1163 Paläontologie, Abhandlungen 219, 207-219. 1164 Pross, J., Houben, A.J.P., Van Simaeys, S., Williams, G.L., Kotthoff, U., Coccioni, R., 1165 Wilpshaar, M., Brinkhuis, H., 2010. Umbria-Marche revisited: A refined 1166 magnetostratigraphic calibration of dinoflagellate cyst events for the 1167 Oligocene of the Western Tethys. Review of Palaeobotany and Palynology 1168 158, 213-235.

1169 Schiøler, P., 2005. Dinoflagellate cysts and acritarchs from the Oligocene-Lower 1170 Miocene interval of the Alma-1X well, Danish North Sea. Journal of 1171 Micropalaeontology 24, 1-37. 1172 Shipboard Scientific Party, 2002. Leg 199 summary. In: Lyle, M., Wilson, P.A., 1173 Janecek, T.R., et al. (Eds.), Proceedings of the Ocean Drilling Program, Initial 1174 Reports, 199, College Station, Texas. 1175 Śliwińska, K.K., Clausen, O., Heilmann-Clausen, C., 2010. A mid-Oligocene cooling 1176 (Oi-2b) reflected in the dinoflagellate record and in depositional sequence 1177 architecture. An integrated study from the eastern North Sea Basin. Marine 1178 and Petroleum Geology 27, 1424-1430. 1179 Śliwińska, K.K., Clausen, O., Heilmann-Clausen, C., 2011. Early Oligocene cooling 1180 reflected by the dinoflagellate cyst Svalbardella cooksoniae. 1181 Palaeogeography, Palaeoclimatology, Palaeoecology 305, 138-149. 1182 Śliwińska, K.K., Abrahamsen, N., Beyer, C., Brünings-Hansen, T., Thomsen, E., 1183 Ulleberg, K., Heilmann-Clausen, C., 2012. Bio-and magnetostratigraphy of 1184 Rupelian—mid Chattian deposits from the Danish land area. Review of 1185 Palaeobotany and Palynology 172, 48-69. 1186 Sluijs, A., Pross, J., Brinkhuis, H., 2005. From greenhouse to icehouse; organic-1187 walled dinoflagellate cysts as paleoenvironmental indicators in the 1188 Paleogene. Earth-Science Reviews 68, 281-315. 1189 St. John, K., 2008. Cenozoic ice-rafting history of the central Arctic Ocean: 1190 Terrigenous sands on the Lomonosov Ridge. Paleoceanography 23, 1-12. 1191 Stickley, C.E., St John, K., Koc, N., Jordan, R.W., Passchier, S., Pearce, R.B., 1192 Kearns, L.E., 2009. Evidence for middle Eocene Arctic sea ice from diatoms and ice-rafted debris. Nature 460, 376-379. 1193 1194 Stover, L.E., 1977. Oligocene and early Miocene dinoflagellates from Atlantic 1195 Corehole 5/5b, Blake Plateau. American Association of Stratigraphic 1196 Palynologists, Contributions Series 5A, 66-89.

1197 Stover, L.E., Hardenbol, J., 1994. Dinoflagellates and depositional sequences in the 1198 lower Oligocene (Rupelian) Boom Clay Formation, Belgium. Bulletin de la 1199 Société Belge de Géologie 102, 5-77. 1200 Stover, L.E., Williams, G.L., 1995. A revision of the Paleogene dinoflagellate genera 1201 Areosphaeridium Eaton 1971 and Eatonicysta Stover and Evitt 1978. 1202 Micropaleontology 41, 97-141. 1203 Tauxe, L., Stickley, C.E., Sugisaki, S., Bijl, P.K., Bohaty, S.M., Brinkhuis, H., Escutia, 1204 C., Flores, J.A., Houben, A.J.P., Iwai, M., Jiménez-Espejo, F., McKay, R., 1205 Passchier, S., Pross, J., Riesselman, C.R., Röhl, U., Sangiorgi, F., Welsh, K., 1206 Klaus, A., Fehr, A., Bendle, J.A.P., Dunbar, R., Gonzàlez, J., Hayden, T., 1207 Katsuki, K., Olney, M.P., Pekar, S.F., Shrivastava, P.K., van de Flierdt, T., 1208 Williams, T., Yamane, M., 2012. Chronostratigraphic framework for the IODP 1209 Expedition 318 cores from the Wilkes Land Margin: constraints for 1210 paleoceanographic reconstruction. Paleoceanography 27, 1-19. 1211 Thomsen, E., Abrahamsen, N., Heilmann-Clausen, C., King, C., Nielsen, O.B., 2012. 1212 Middle Eocene to earliest Oligocene development in the eastern North Sea 1213 Basin: Biostratigraphy, magnetostratigraphy and palaeoenvironment of the 1214 Kysing-4 borehole, Denmark. Palaeogeography, Palaeoclimatology, 1215 Palaeoecology 350-352, 212-235. 1216 Torricelli, S., Biffi, U., 2001. Palynostratigraphy of the Numidian Flysch of Northern 1217 Tunisia (Oligocene-early Miocene). Palynology 25, 29-55. 1218 Van Mourik, C.A.B., Brinkhuis, H., 2000. Data report: Organic-walled dinoflagellate 1219 cyst biostratiraphy of the latest middle to late Eocene at Hole 1053A 1220 (subtropical Atlantic Ocean). In: Kroon, D., Norris, R.D., Klaus, A. (Eds.), 1221 Proceedings of the Integrated Ocean Drilling Program, Scientific Results Vol. 1222 171B, pp.1-25. 1223 Van Mourik, C.A., Brinkhuis, H., 2005. The Massignano Eocene-Oligocene golden 1224 spike section revisited. Stratigraphy 2, 13-30.

1225 Van Peer, T.E., Liebrand, D., Xuan, C., Lippert, P.C., Angini, C., Blum, P., Bown, 1226 P.R., Greenop, R., Kordesch, W.E.C., Leonhardt, D., Friedrich, O., Wilson, 1227 P.A., in press. Revised composite depth scale, splice and magnetic 1228 stratigraphy for IODP Site U1406. In Norris, R.D., Wilson, P.A., Blum, P., and 1229 the Expedition 342 Scientists (Eds.), Proceedings of the Integrated Ocean 1230 Drilling Program 342, College Station, Texas. 1231 Van Simaeys, S., De Man, E., Vandenberghe, N., Brinkhuis, H., Steurbaut, E., 2004. 1232 Stratigraphic and palaeoenvironmental analysis of the Rupelian–Chattian 1233 transition in the type region: evidence from dinoflagellate cysts, foraminifera 1234 and calcareous nannofossils. Palaeogeography, Palaeoclimatology, 1235 Palaeoecology 208, 31-58. 1236 Van Simaeys, S., Munsterman, D., Brinkhuis, H., 2005a. Oligocene dinoflagellate 1237 cyst biostratigraphy of the southern North Sea Basin. Review of Palaeobotany and Palynology 134, 105-128. 1238 1239 Van Simaeys, S., Brinkhuis, H., Pross, J., Williams, G.L., Zachos, J.C., 2005b. Arctic 1240 dinoflagellate migrations mark the strongest Oligocene glaciations. Geology 1241 33, 709-712. 1242 Via, R.K., Thomas, D.J., 2006. Evolution of Atlantic thermohaline circulation: Early 1243 Oligocene onset of deep-water production in the North Atlantic. Geology 34, 1244 441-444. 1245 Wade, B.S., Kroon, D., Norris, R.D., 2001. Orbitally forced climate change in late 1246 mid-Eocene time at Blake Nose (Leg 171B): evidence from stable isotopes in 1247 foraminifera. Geological Society, London, Special Publications 183, 273-291. 1248 Wade, B.S., Pälike, H., 2004. Oligocene climate dynamics. Paleoceanography 19, 1249 PA4019. 1250 Williams, G.L., Bujak, J.P., 1977: Cenozoic palynostratigraphy of offshore eastern 1251 Canada. American Associantion of Stratigraphic Palynologists, Contribution 1252 Series A5, 14-47.

1253	Williams, G.L., Bujak, J.P., 1985. Mesozoic and Cenozoic dinoflagellates. In: Bolli,
1254	H.M., Saunders, J.B., Perch-Nielsen, K. (Eds.), Plankton Stratigraphy.
1255	Cambridge University Press, Cambridge, pp. 847-964.
1256	Williams, G.L., Manum, S.B., 1999. Oligocene-Early Miocene dinocyst stratigraphy of
1257	Hole 985A (Norwegian Sea). In: Raymo, M.E., Jansen, E., Blum, P., Herbert,
1258	T.D. (Eds.), Proceedings of the Integrated Ocean Drilling Program, Scientific
1259	Results 162, 99-109.
1260	Williams, G.L., Brinkhuis, H., Pearce, M.A., Fensome, R.A., Weegink, J.W., 2004.
1261	Southern Ocean and global dinoflagellate cyst events compared: index
1262	events for the Late Cretaceous-Neogene. In: Exon, N.F., Kennett, J.P.,
1263	Malone, M.J. (Eds.), Proceedings of the Integrated Ocean Drilling Program,
1264	Scientific Results 189, 1-98.
1265	Wilpshaar, M., Santarelli, A., Brinkhuis, H., Visscher, H., 1996. Dinoflagellate cysts
1266	and mid-Oligocene chronostratigraphy in the central Mediterranean region.
1267	Journal of the Geological Society 153, 553-561.
1268	Zachos, J.C., Dickens, G.R., Zeebe, R.E., 2008. An early Cenozoic perspective on
1269	greenhouse warming and carbon-cycle dynamics. Nature 451, 279-283.

1270 Figure captions 1271 1272 Figure 1: Compilation of magnetostratigraphically-calibrated dinocyst 1273 biostratigraphies available for the North Atlantic, North Sea, and the western Tethys 1274 region. 1275 1276 Figure 2: Geographical map of the North Atlantic region, with locations of studied 1277 sites (star) and locations of other dinocyst studies discussed in the text. 1 – Fensome 1278 et al. (2009); 2 – Head and Norris (1989); 3 – Eldrett et al. (2004); 4 – Manum 1279 (1976); Williams and Manum (1999); 5 – Bujak and Mudge (1994); 6 – Śliwińska et 1280 al. (2012); 7 – Heilmann-Clausen and Van Simaeys (2005), Thomsen et al. (2012); 8 1281 - Schiøler (2005), Dybkjær et al. (2012); 9 - Van Simaeys et al. (2004), Van 1282 Simaeys et al. (2005); 10 - Munsterman and Brinkhuis (2004); 11 - Kempf and 1283 Pross (2005); 12 – Biffi and Manum (1988), Brinkhuis and Biffi (1993), Wilpshaar et 1284 al. (1996), Pross et al. (2010). 1285 1286 Figure 3: Semiguantitative range chart of dinocyst taxa encountered at Site U1405 of 1287 IODP Expedition 342, including shipboard-generated magnetostratigraphy and 1288 Calcareous Nannoplankton Zonation (Norris et al., 2014d). 1289 Figure 4: Semiquantitative range chart of dinocyst taxa encountered at Site U1406 of 1290 1291 IODP Expedition 342, plotted on revised composite depth scale (revised CCSF-A) 1292 and including revised magnetostratigraphy (Van Peer et al., in press), and shipboard 1293 Calcareous Nannoplankton Zonation (Norris et al., 2014c). 1294 1295 Figure 5: Semiquantitative range chart of dinocyst taxa encountered at Site U1411 of 1296 IODP Expedition 342, including shipboard-generated magnetostratigraphy and 1297 Calcareous Nannoplankton Zonation (Norris et al., 2014b).

1298 1299 Figure 6: Semiquantitative range chart of dinocyst taxa encountered at Site U1411 of 1300 IODP Expedition 342, including shipboard-generated magnetostratigraphy and 1301 Calcareous Nannoplankton Zonation (Norris et al., 2014b). 1302 1303 Figure 7: Integrated scheme of magnetostratigraphically-calibrated dinocyst events 1304 for the uppermost Eocene to lowermost Miocene of the Newfoundland Margin based 1305 on the observations from IODP Sites U1405, U1406 and U1411. Time scale, 1306 magnetostratigraphy, and Calcareous Nannoplankton Zones after Gradstein et al. 1307 (2012).1308 1309 **Table captions** 1310 1311 Table 1: Compilation of magnetostratigraphically-calibrated dinocyst FADs as known 1312 from different regions in the Northern Hemisphere for the latest Eocene to earliest 1313 Miocene. Data are from Eldrett et al. (2004) for the Norwegian-Greenland Sea, 1314 Williams and Manum (1999) for the Norwegian Sea, Śliwińska et al. (2012) for the 1315 Danish land area, and Pross et al. (2010) for the Umbria-Marche region of Central 1316 Italy. Given ages refer to Gradstein et al. (2012). 1317 1318 Table 2: Compilation of magnetostratigraphically-calibrated dinocyst LADs as known 1319 from different regions in the Northern Hemisphere for the latest Eocene to earliest 1320 Miocene. Data are from Eldrett et al. (2004) for the Norwegian-Greenland Sea, 1321 Williams and Manum (1999) for the Norwegian Sea, Śliwińska et al. (2012) for the 1322 Danish land area, and Pross et al. (2010) and Wilpshaar et al. (1996; marked by *) 1323 for the Umbria-Marche region of Central Italy. Given ages refer to Gradstein et al. 1324 (2012).

1325

1326	Appendix A	, Table A.1
1327	Alphabetica	I list of all identified taxa, key to their occurrences in the range charts
1328	(Figs. 3–6), a	and key to positions of respective photomicrographs in Plates I to VIII.
1329		
1330		
1331	Plate captio	ons
1332		
1333	Plate I: Scal	e bar = 20 μm applies to all figures; all photographs taken using
1334	differential in	iterference contrast.
1335	1, 2	Apteodinium australiense (Deflandre and Cookson, 1955) Williams,
1336		1978; Sample U1406 A17 H4 84-86 cm; Slide 14G394 A; England
1337		Finder coordinates L36/2; specimen in high and low focus.
1338	3	Apteodinium spiridoides Benedek, 1972; Sample U1406 B13 H3 84-
1339		86 cm; Slide 14G494 A; T17.
1340	4	Areoligera semicirculata (Morgenroth, 1966b) Stover and Evitt, 1978
1341		Sample U1406 C16 H6 76-78 cm; P46.
1342	5	Areosphaeridium diktyoplokum (Klumpp, 1953) Eaton, 1971; Sample
1343		U1411 B17 H3 126-128 cm; Slide 15A82 A; P26/2.
1344	6	Artemisiocysta cladodichotoma Benedek, 1972; Sample U1405 B19
1345		H5 136-138 cm; Slide 14L220; S28.
1346	7	Batiacasphaera micropapillata Stover, 1977; Sample U1406 B11 H3
1347		84-86 cm; Slide 14G404 A; N25/3.
1348	8, 9	Cerebrocysta bartonensis Bujak in Bujak et al., 1980; Sample U1411
1349		C12 X3 113-115 cm; Slide 15A234 A; S35/1; specimen in high and
1350		low focus.
1351		
1352	Plate II: Sca	le bar = 20 μm applies to all figures; all photographs taken using
1353	differential in	iterference contrast.

1354	1	Cordosphaeridium minimum (Morgenroth, 1966a) Benedek, 1972;
1355		Sample U1406 A19 H3 84-86 cm; Slide 14G398 A; England Finder
1356		coordinates P25/3.
1357	2, 3	Corrudinium incompositum (Drugg, 1970b) Stover and Evitt, 1978;
1358		Sample U1411 B17 H3 126-128 cm; Slide 15A82 A; G40/3; specimen
1359		in high and low focus.
1360	4	Cyclodictyon spp.; Sample U1406 C18 H5 76-79 cm; Slide A; C41.
1361	5, 6	Chiropteridium galea (Maier, 1959) Sarjeant, 1983; Sample U1406
1362		B17 H3 84-86 cm; Slide 14H44 A; U19; specimen in high and low
1363		focus.
1364	7, 8	Chiropteridium lobospinosum Gocht, 1960; Sample U1406 B14 H3 84-
1365		86 cm; Slide 14G498 A; W17; specimen in high and low focus.
1366		
1367	Plate III: Sca	le bar = 20 μm applies to all figures; photographs taken using
1368	differe	ential interference contrast.
1368 1369	differe	ential interference contrast. Cordosphaeridium cf. funiculatum sensu Biffi and Manum, 1988;
1369		Cordosphaeridium cf. funiculatum sensu Biffi and Manum, 1988;
1369 1370	1	Cordosphaeridium cf. funiculatum sensu Biffi and Manum, 1988; Sample U1411 C9 H4 59-61 cm; Slide 15A181; R17/3.
1369 1370 1371	1	Cordosphaeridium cf. funiculatum sensu Biffi and Manum, 1988; Sample U1411 C9 H4 59-61 cm; Slide 15A181; R17/3. Cordosphaeridium cantharellus (Brosius, 1963) Gocht, 1969; Sample
1369 1370 1371 1372	1	Cordosphaeridium cf. funiculatum sensu Biffi and Manum, 1988; Sample U1411 C9 H4 59-61 cm; Slide 15A181; R17/3. Cordosphaeridium cantharellus (Brosius, 1963) Gocht, 1969; Sample U1406 B17 H3 84-86 cm; Slide 14H44 A; U31/2; specimen in high
1369 1370 1371 1372 1373	2, 3	Cordosphaeridium cf. funiculatum sensu Biffi and Manum, 1988; Sample U1411 C9 H4 59-61 cm; Slide 15A181; R17/3. Cordosphaeridium cantharellus (Brosius, 1963) Gocht, 1969; Sample U1406 B17 H3 84-86 cm; Slide 14H44 A; U31/2; specimen in high and low focus.
1369 1370 1371 1372 1373 1374	2, 3	Cordosphaeridium cf. funiculatum sensu Biffi and Manum, 1988; Sample U1411 C9 H4 59-61 cm; Slide 15A181; R17/3. Cordosphaeridium cantharellus (Brosius, 1963) Gocht, 1969; Sample U1406 B17 H3 84-86 cm; Slide 14H44 A; U31/2; specimen in high and low focus. Dapsilidinium pseudocolligerum (Stover, 1977) Bujak et al., 1980;
1369 1370 1371 1372 1373 1374 1375	1 2, 3 4	Cordosphaeridium cf. funiculatum sensu Biffi and Manum, 1988; Sample U1411 C9 H4 59-61 cm; Slide 15A181; R17/3. Cordosphaeridium cantharellus (Brosius, 1963) Gocht, 1969; Sample U1406 B17 H3 84-86 cm; Slide 14H44 A; U31/2; specimen in high and low focus. Dapsilidinium pseudocolligerum (Stover, 1977) Bujak et al., 1980; Sample U1406 A18 H2 84-86 cm; Slide 14G396 C; S17.
1369 1370 1371 1372 1373 1374 1375 1376	1 2, 3 4	Cordosphaeridium cf. funiculatum sensu Biffi and Manum, 1988; Sample U1411 C9 H4 59-61 cm; Slide 15A181; R17/3. Cordosphaeridium cantharellus (Brosius, 1963) Gocht, 1969; Sample U1406 B17 H3 84-86 cm; Slide 14H44 A; U31/2; specimen in high and low focus. Dapsilidinium pseudocolligerum (Stover, 1977) Bujak et al., 1980; Sample U1406 A18 H2 84-86 cm; Slide 14G396 C; S17. Dinopterygium cladoides Deflandre, 1935; Sample U1411 A17 H4 84-
1369 1370 1371 1372 1373 1374 1375 1376 1377	1 2, 3 4 5	Cordosphaeridium cf. funiculatum sensu Biffi and Manum, 1988; Sample U1411 C9 H4 59-61 cm; Slide 15A181; R17/3. Cordosphaeridium cantharellus (Brosius, 1963) Gocht, 1969; Sample U1406 B17 H3 84-86 cm; Slide 14H44 A; U31/2; specimen in high and low focus. Dapsilidinium pseudocolligerum (Stover, 1977) Bujak et al., 1980; Sample U1406 A18 H2 84-86 cm; Slide 14G396 C; S17. Dinopterygium cladoides Deflandre, 1935; Sample U1411 A17 H4 84-86 cm; Slide 14G394 A; T25/1.
1369 1370 1371 1372 1373 1374 1375 1376 1377	1 2, 3 4 5	Cordosphaeridium cf. funiculatum sensu Biffi and Manum, 1988; Sample U1411 C9 H4 59-61 cm; Slide 15A181; R17/3. Cordosphaeridium cantharellus (Brosius, 1963) Gocht, 1969; Sample U1406 B17 H3 84-86 cm; Slide 14H44 A; U31/2; specimen in high and low focus. Dapsilidinium pseudocolligerum (Stover, 1977) Bujak et al., 1980; Sample U1406 A18 H2 84-86 cm; Slide 14G396 C; S17. Dinopterygium cladoides Deflandre, 1935; Sample U1411 A17 H4 84-86 cm; Slide 14G394 A; T25/1. Cribroperidinium sp.1; Sample U1411 B17 H3 126-128 cm; Slide

1382	10	Enneadocysta magna Fensome et al., 2006; Sample U1406 A19 H3
1383		84-86 cm; Slide 14G398 A; G30.
1384		
1385	Plate IV: Sca	le bar = 20 μm applies to all figures; all photographs taken using
1386	differe	ntial interference contrast.
1387	1	Deflandrea phosphoritica Eisenack, 1938b; Sample U1411 C7 H6 6-8
1388		cm; Slide 15A178 B; England Finder coordinates S44/3.
1389	2	Charlesdowniea clathrata (Eisenack, 1938b) Lentin and
1390		Vozzhennikova, 1989; Sample U1411 B18 H2 123-125 cm; Slide
1391		15A172 A; T27.
1392	3	Enneadocysta pectiniformis (Gerlach, 1961) Stover and Williams;
1393		Sample U1411 C11 X5 133-135 cm; Slide 15A232 A; S18.
1394	4	Gelatia inflata Bujak, 1984; Sample U1406 A18 H3 84-86 cm; Slide
1395		14G397 B; R39/2.
1396	5	Hemiplacophora semilunifera Cookson and Eisenack, 1965a; Sample
1397		U1411 C9 H4 59-61 cm; Slide 15A181 A; R40.
1398	6, 7	Filisphaera filifera Bujak, 1984; Sample U1406 B14 H3 84-86 cm;
1399		Slide 14G498 A; T28/2; specimen in high and low focus.
1400	8, 9	Impagidinium sp.; Sample U1411 C9 H4 59-61 cm; Slide 15A181 A;
1401		S43; specimen in high and low focus.
1402		
1403	Plate V: Scale	e bar = 20 μm applies to all figures; all photographs taken using
1404	differe	ntial interference contrast.
1405	1	Glaphyrocysta semitecta (Bujak in Bujak et al., 1980) Lentin and
1406		Williams, 1981; Sample U1411 B16 H4 41-43 cm; Slide 15A80 A;
1407		England Finder coordinates U24/1.
1408	2	Glaphyrocysta sp.; Sample U1406 B17 H3 76-79 cm; Slide 14H44 A;
1409		U31/2.

1410	3	Homotryblium plectilum Drugg and Löblich Jr., 1976; Sample U1406
1411		A17 H4 84-86 cm; Slide 14G394 A; S30/3.
1412	4	Hystrichokolpoma pusillum Biffi and Manum, 1988; Sample U1406
1413		B13 H3 84-86 cm; Slide 14G494 C; J24/1.
1414	5	Oligokolpoma sp.; Sample U1406 A19 H5 84-86 cm; Slide 14G400
1415		B; H34/2.
1416	6, 7	Hystrichokolpoma rigaudiae Deflandre and Cookson, 1955; Sample
1417		U1411 C9 H4 59-61 cm; Slide 15A181 A; G32; specimen in high and
1418		low focus.
1419	8	Hystrichokolpoma cinctum Klumpp, 1953; Sample U1406 C16 H6 84-
1420		86 cm; Slide 14H113 A; T13.
1421		
1422	Plate VI: Sca	le bar = 20 μm applies to all figures; all photographs taken using
1423	differe	ential interference contrast.
1424	1	Impletosphaeridium insolitum Eaton, 1976; Sample U1405 C17 H2
1425		94-96 cm; Slide 14L228 A; England Finder coordinates P13/4.
1.40.6		
1426	2	Lejeunecysta fallax (Morgenroth, 1966b) Artzner and Dörhöfer, 1978;
1426	2	Lejeunecysta fallax (Morgenroth, 1966b) Artzner and Dörhöfer, 1978; Sample U1405 B21 H3 12-14 cm; Slide 14L222A; G18/3.
	3, 4	
1427		Sample U1405 B21 H3 12-14 cm; Slide 14L222A; G18/3.
1427 1428		Sample U1405 B21 H3 12-14 cm; Slide 14L222A; G18/3. Lentinia serrata Bujak in Bujak et al., 1980; Sample U1411 B16 H4
1427 1428 1429	3, 4	Sample U1405 B21 H3 12-14 cm; Slide 14L222A; G18/3. Lentinia serrata Bujak in Bujak et al., 1980; Sample U1411 B16 H4 41-43 cm; Slide 15A80 A; T41; specimen in high and low focus.
1427 1428 1429 1430	3, 4	Sample U1405 B21 H3 12-14 cm; Slide 14L222A; G18/3. Lentinia serrata Bujak in Bujak et al., 1980; Sample U1411 B16 H4 41-43 cm; Slide 15A80 A; T41; specimen in high and low focus. Lingulodinium machaerophorum (Deflandre and Cookson, 1955) Wall,
1427 1428 1429 1430 1431	3, 4 5	Sample U1405 B21 H3 12-14 cm; Slide 14L222A; G18/3. Lentinia serrata Bujak in Bujak et al., 1980; Sample U1411 B16 H4 41-43 cm; Slide 15A80 A; T41; specimen in high and low focus. Lingulodinium machaerophorum (Deflandre and Cookson, 1955) Wall, 1967; Sample U1406 B14 H3 84-86 cm; Slide 14G498 A; O20/4.
1427 1428 1429 1430 1431 1432	3, 4 5	Sample U1405 B21 H3 12-14 cm; Slide 14L222A; G18/3. Lentinia serrata Bujak in Bujak et al., 1980; Sample U1411 B16 H4 41-43 cm; Slide 15A80 A; T41; specimen in high and low focus. Lingulodinium machaerophorum (Deflandre and Cookson, 1955) Wall, 1967; Sample U1406 B14 H3 84-86 cm; Slide 14G498 A; O20/4. Lophocysta sulcolimbata Manum, 1979; Sample U1411 B15 H4 0-2
1427 1428 1429 1430 1431 1432 1433	3, 4 5 6, 7	Sample U1405 B21 H3 12-14 cm; Slide 14L222A; G18/3. Lentinia serrata Bujak in Bujak et al., 1980; Sample U1411 B16 H4 41-43 cm; Slide 15A80 A; T41; specimen in high and low focus. Lingulodinium machaerophorum (Deflandre and Cookson, 1955) Wall, 1967; Sample U1406 B14 H3 84-86 cm; Slide 14G498 A; O20/4. Lophocysta sulcolimbata Manum, 1979; Sample U1411 B15 H4 0-2 cm; Slide 15A78 A; N38; specimen in high and low focus.
1427 1428 1429 1430 1431 1432 1433 1434	3, 4 5 6, 7	Sample U1405 B21 H3 12-14 cm; Slide 14L222A; G18/3. Lentinia serrata Bujak in Bujak et al., 1980; Sample U1411 B16 H4 41-43 cm; Slide 15A80 A; T41; specimen in high and low focus. Lingulodinium machaerophorum (Deflandre and Cookson, 1955) Wall, 1967; Sample U1406 B14 H3 84-86 cm; Slide 14G498 A; O20/4. Lophocysta sulcolimbata Manum, 1979; Sample U1411 B15 H4 0-2 cm; Slide 15A78 A; N38; specimen in high and low focus. Melitasphaeridium asterium (Eaton, 1976) Bujak et al., 1980; Sample

1438	10, 11	Oligokolpoma galeottii Pross et al., 2010; Sample U1406 A19 H3 84-
1439		86 cm; Slide 14G398 A; S21/3; specimen in high and low focus.
1440	12, 13, 14	Nematosphaeropsis labyrinthus (Ostenfeld, 1903) Reid, 1974; Sample
1441		U1406 A22 H4 38-40 cm; Slide 15A4A; S34/4; specimen in high and
1442		low focus.
1443		
1444	Plate VII: Sca	le bar = 20 μm applies to all figures; all photographs taken using
1445	differe	ntial interference contrast.
1446	1	Operculodinium centrocarpum Deflandre and Cookson, 1955) Wall,
1447		1976; Sample U1406 A17 H4 84-86 cm; Slide 14G394 B; England
1448		Finder coordinates M27/1.
1449	2	Phthanoperidinium comatum (Morgenroth, 1966b) Eisenack and
1450		Kjellström, 1972; Sample U1411 B15 H4 0-2 cm; Slide 15A78 A; P24.
1451	3	Reticulatosphaera actinocoronata (Benedek, 1972) Bujak and
1452		Matsuoka, 1986; Sample U1406 B14 H3 84-86 cm; Slide 14G498 A;
1453		S19.
1454	4	Saturnodinium pansum (Stover, 1977) Brinkhuis et al., 1992; Sample
1455		U1406 C16 H5 76-78 cm; Slide A; J42/2.
1456	5	Rhombodinium draco Gocht, 1955; Sample U1411 C8 H4 146-148
1457		cm; Slide 15A180A; V28/2.
1458	6	Spiniferites manumii (Lund, 2002) Schiøler, 2005; Sample U1406 A22
1459		H4 38-40 cm; Slide 15A4 A; H38/2.
1460	7	Spiniferites pseudofurcatus (Klumpp, 1953) Sarjeant, 1970; Sample
1461		U1406 B11 H5 84-86 cm; Slide 14G487A; T34.
1462	8	Pentadinium laticinctum Gerlach, 1961; Sample U1406 A17 H5 84-86
1463		cm; Slide 14G395 C; P22.
1464	9	Schematophora speciosa Deflandre and Cookson, 1955; Sample
1465		U1411 B18 H2 123-125 cm; Slide 15A172 A; F28/1.

1466	10, 11	Stoveracysta sp. 1; Sample U1411 C8 H4 146-148 cm; Slide 15A180
1467		A; P28; specimen in high and low focus.
1468	12	Svalbardella sp. 1; Sample U1411 C8 H4 146-148 cm; Slide 15A180
1469		A; H44/3.
1470	13	Svalbardella sp. 2; Sample U1406 A19 H5 84-86 cm; Slide 14G400 A;
1471		W33.
1472	14	Svalbardella sp. 3; Sample U1406 A19 H 3 84-86 cm; Slide 14G398
1473		A; U14.
1474	15	Palaeocystodinium golzowense Alberti, 1961; Sample U1411 B15 H4
1475		0-2 cm; Slide 15A78 A; Q23/4.
1476		
1477	Plate VIII: Sc	ale bar = 20 µm applies to all figures; all photographs taken using
1478	differe	ential interference contrast.
1479	1	Selenopemphix crenata Matsuoka and Bujak, 1988; Sample U1411
1480		C8 H4 146-148 cm; Slide 15A180 A; England Finder coordinates F33.
1481	2	Selenopemphix nephroides Benedek, 1972; Sample U1411 C8 H4
1482		146-148 cm; Slide 15A180 A; N33/4.
1483	3, 4	Tectatodinium pellitum Wall, 1967; Sample U1406 A17 H4 84-86 cm;
1484		Slide 14G394 B; T39/4; specimen in high and low focus.
1485	5	Thalassiphora delicata Williams and Downie, 1966c; Sample U1411
1486		C8 H4 146-148 cm; Slide 15A180 B; W22.
1487	6	Wetzeliella gochtii Costa and Downie, 1976; Sample U1406 A19 H3
1488		84-86 cm; Slide 14G398 B; V42.
1489	7	Wetzeliella symmetrica Weiler, 1956; Sample U1406 A19 H4 80-83
1490		cm; N32.
1491	8, 9	Thalassiphora pelagica (Eisenack, 1954b) Eisenack and
1492		Gocht, 1960; Sample U1406 A17 H5 84-86 cm; Slide 14G395 C; Q34;
1493		specimen in high and low focus.

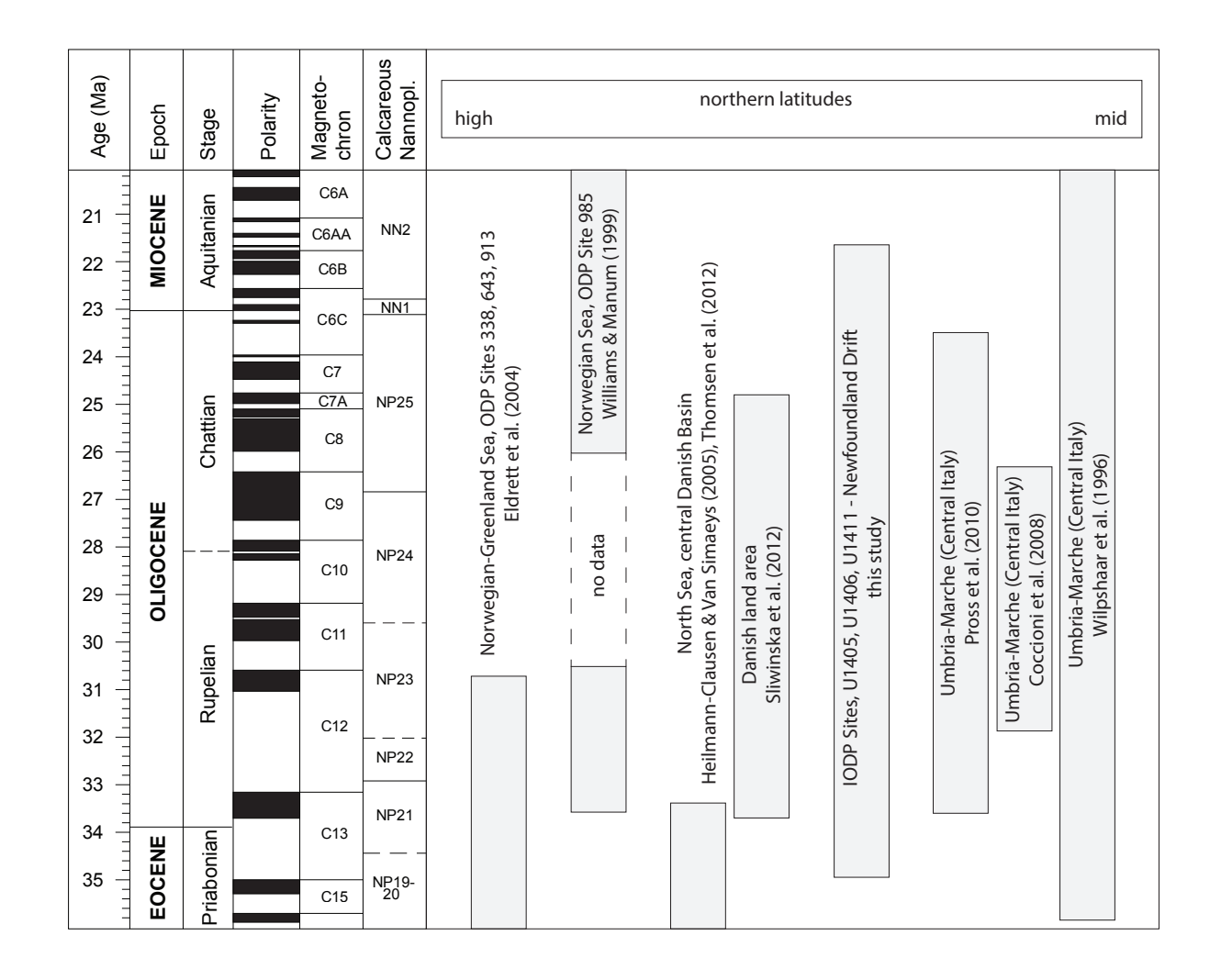


Fig. 2

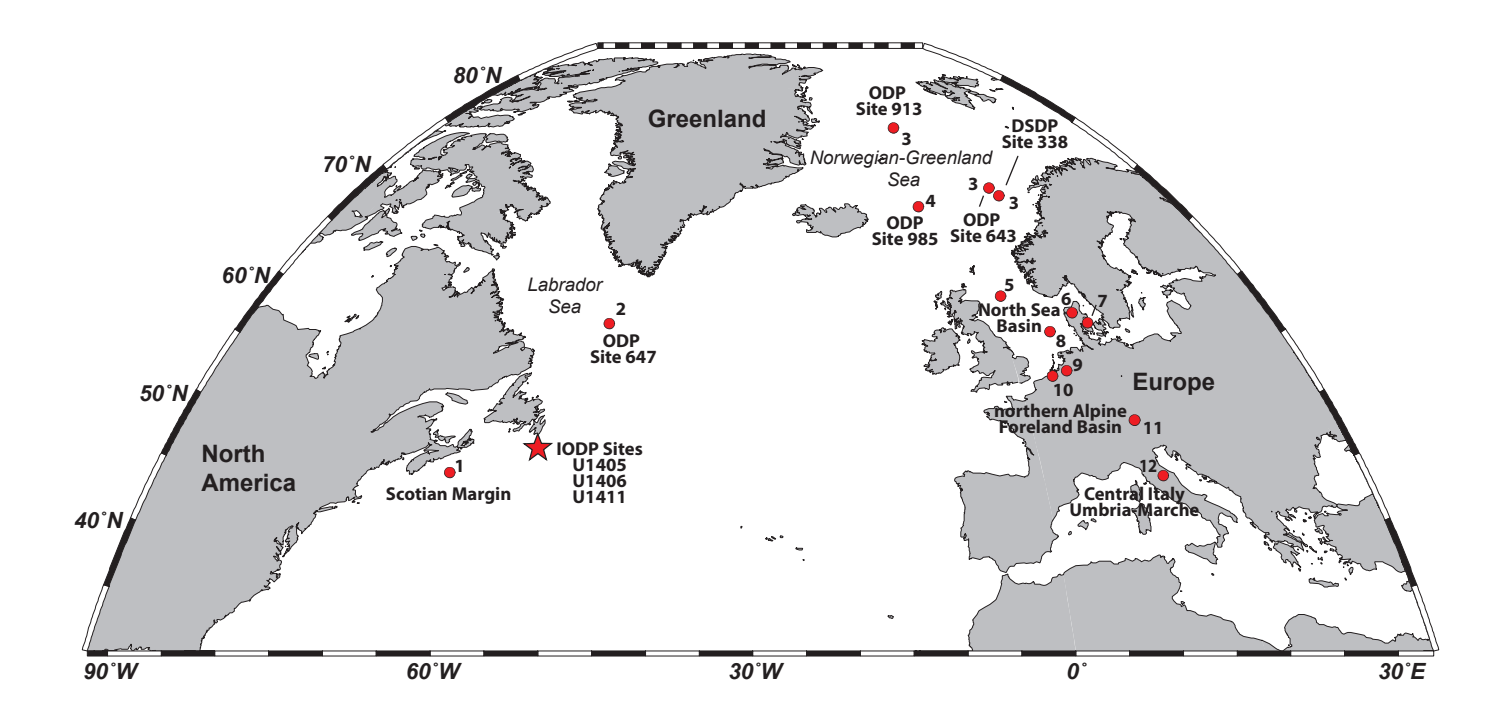
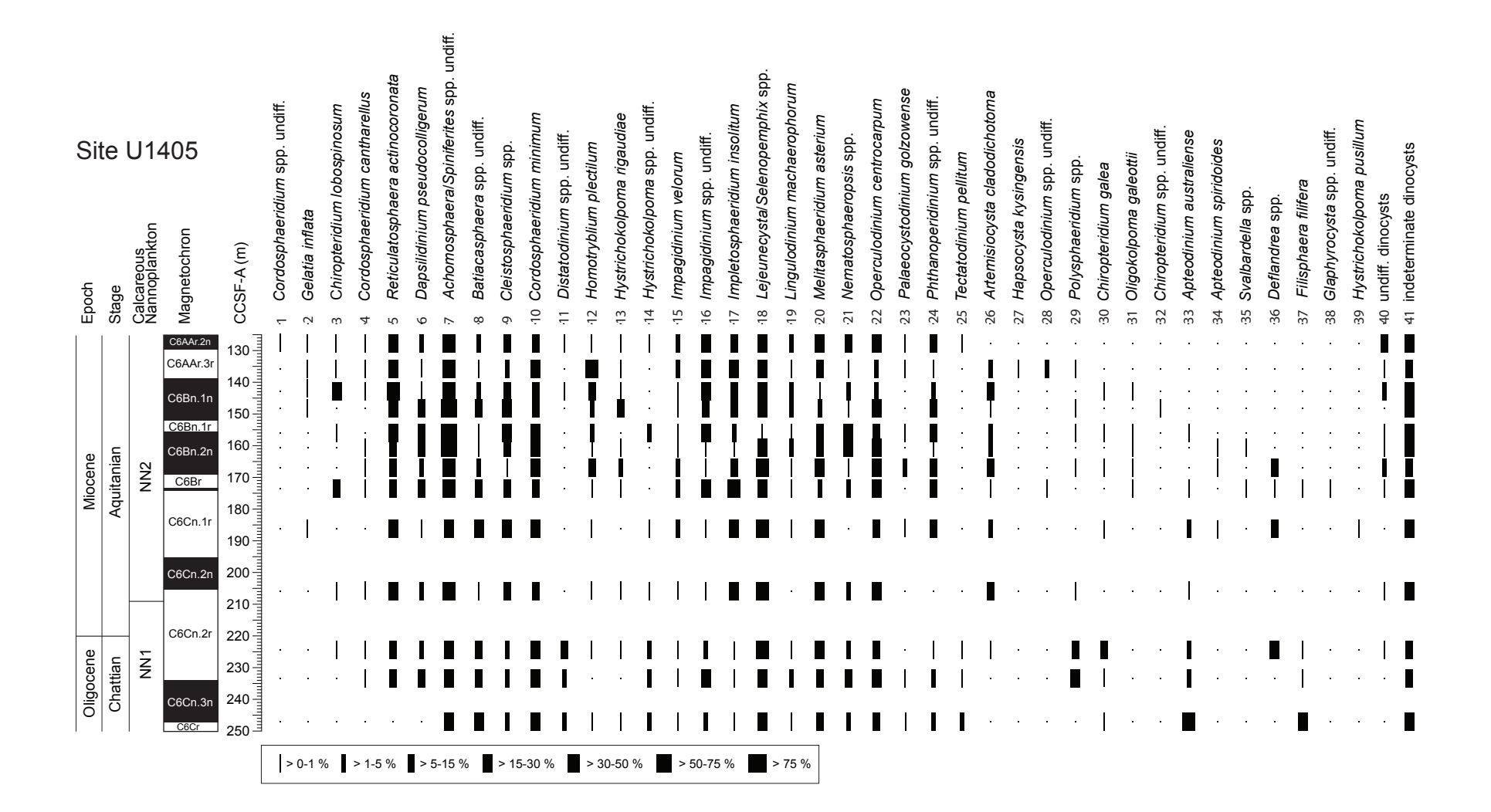


Fig. 3



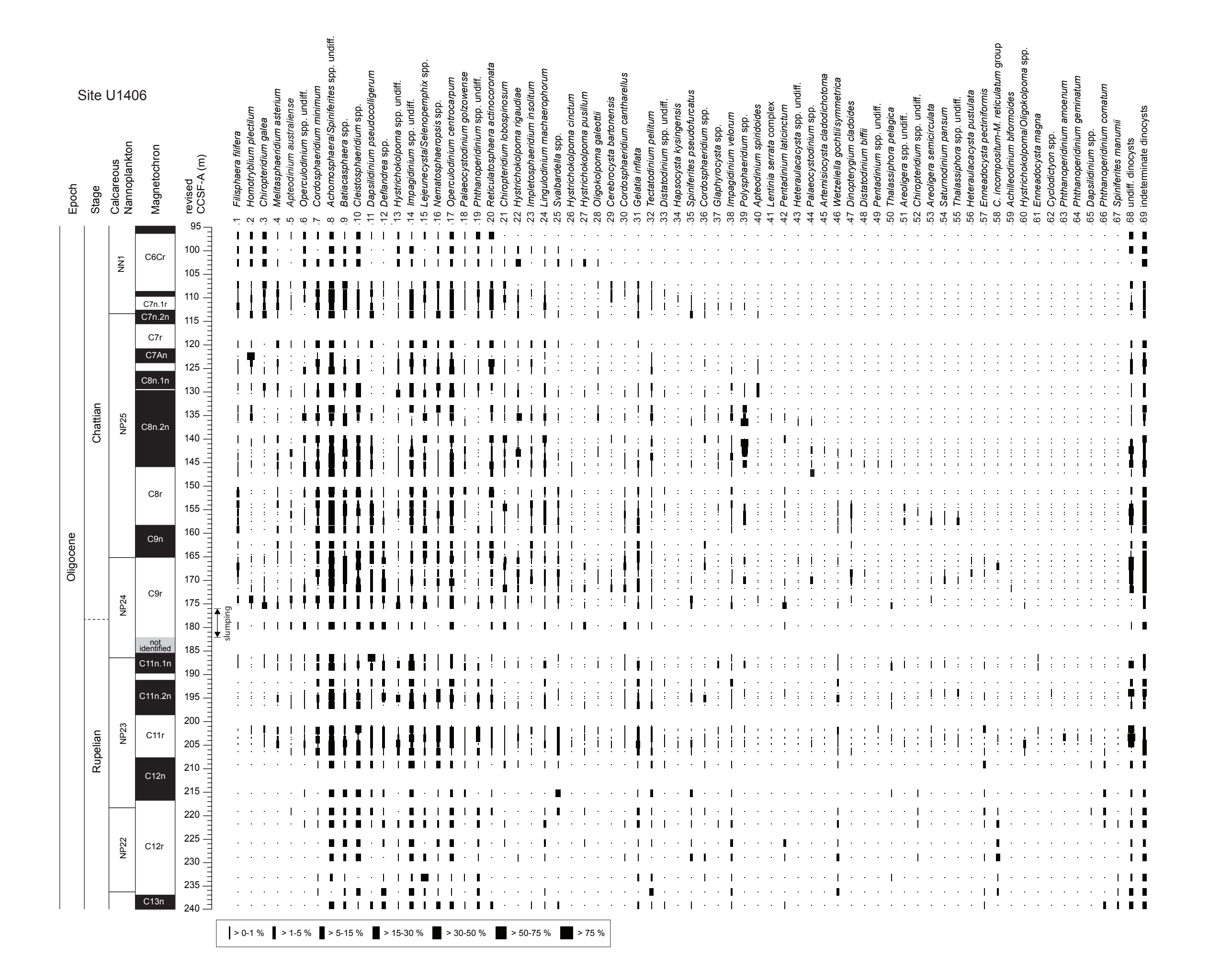
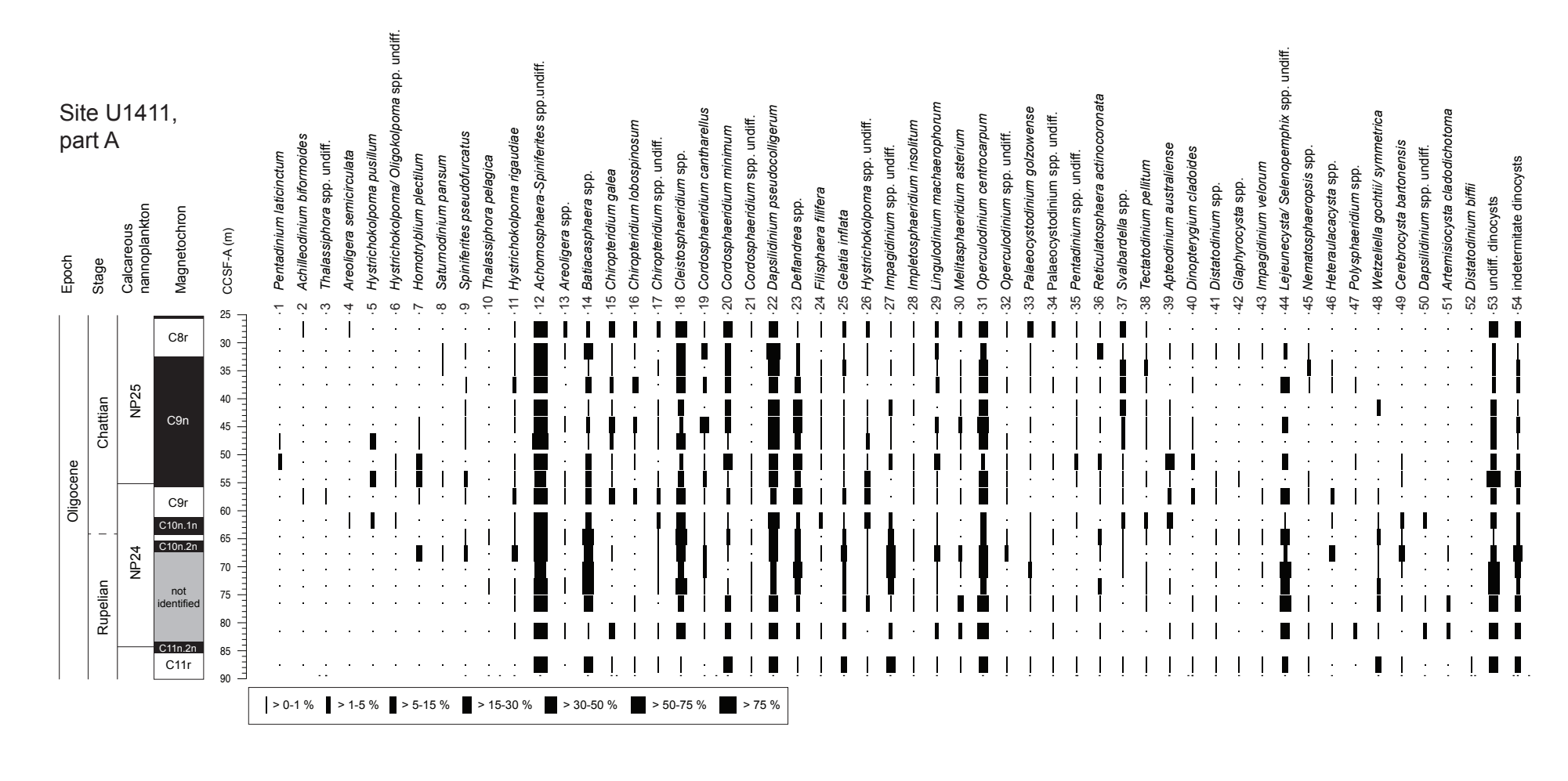
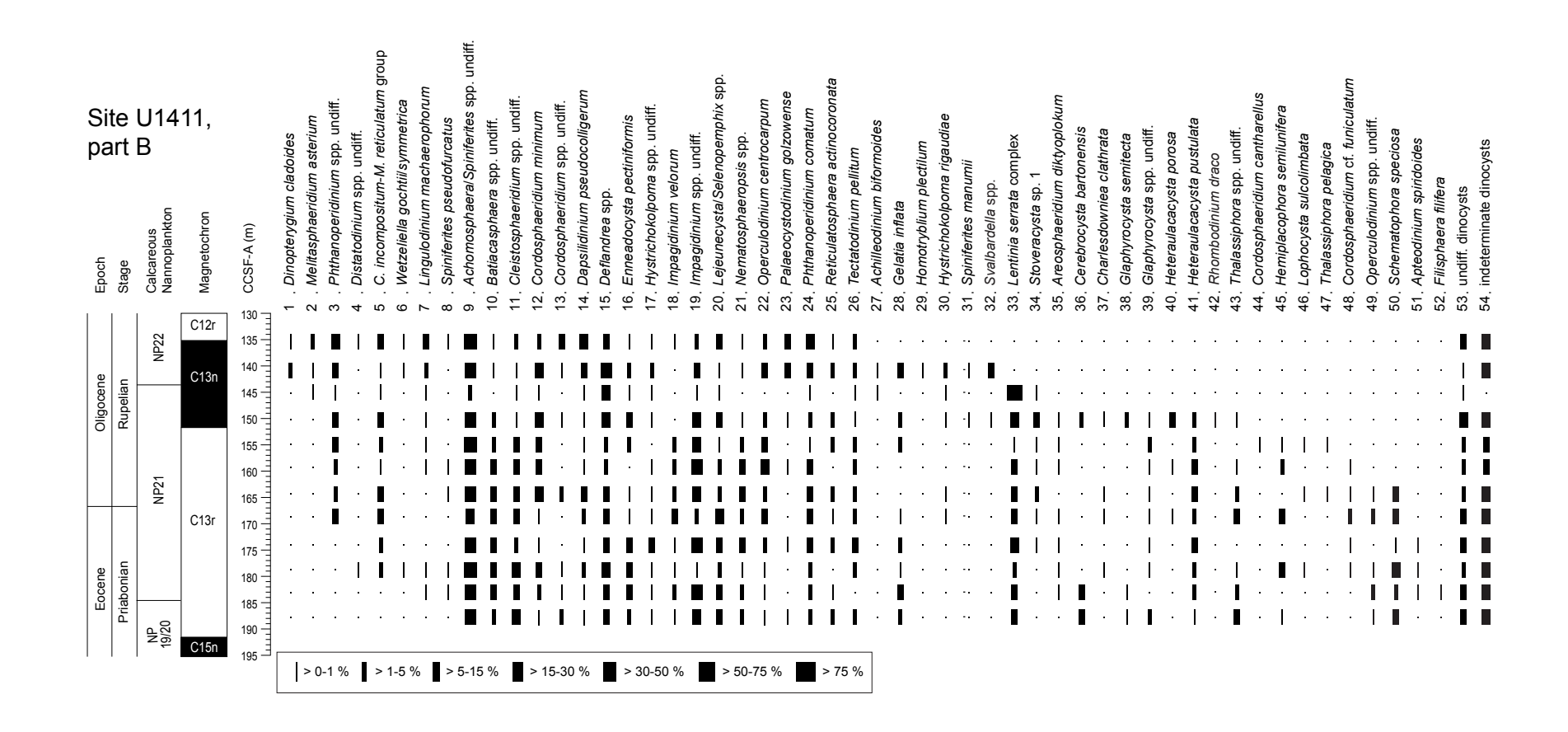
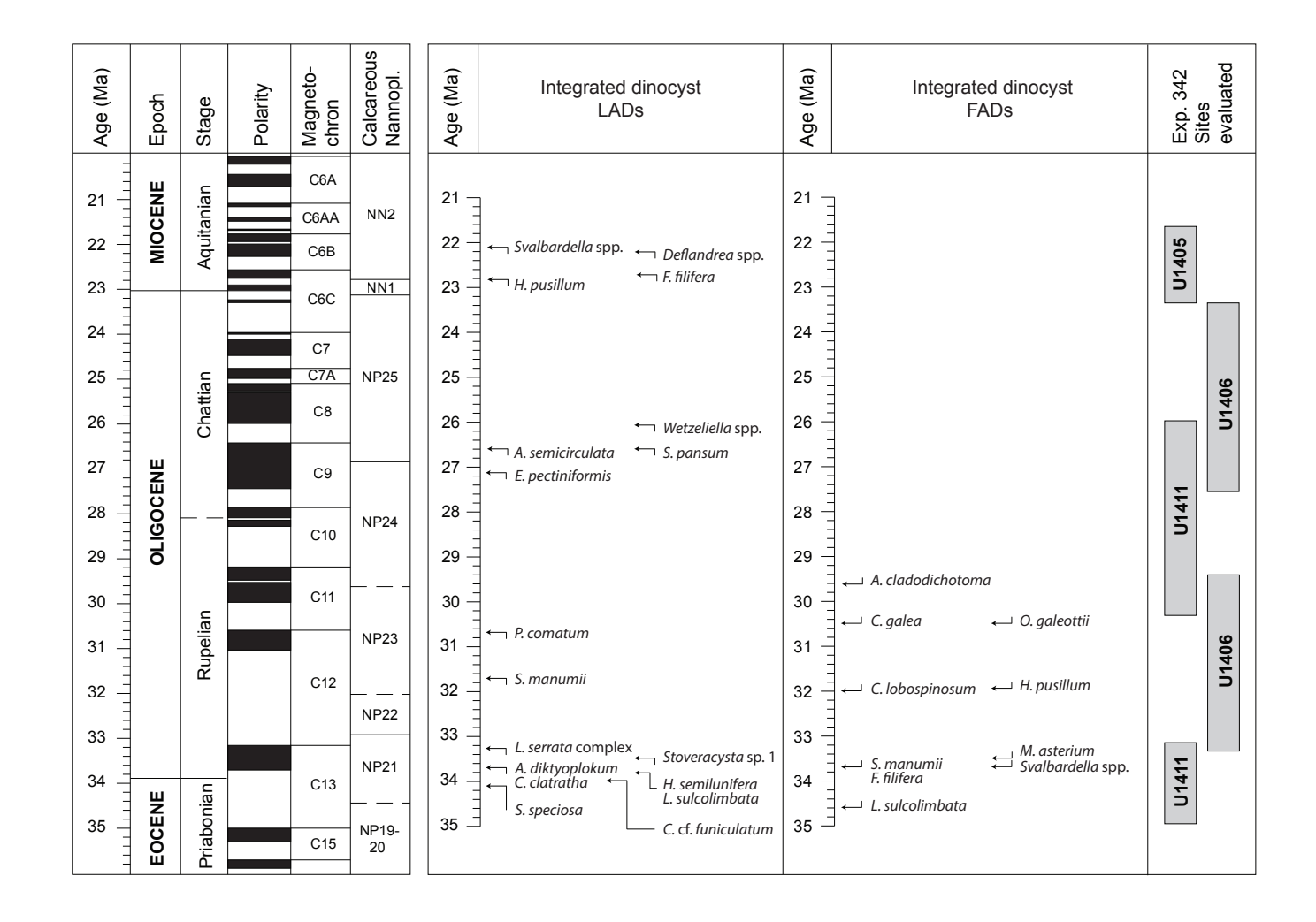
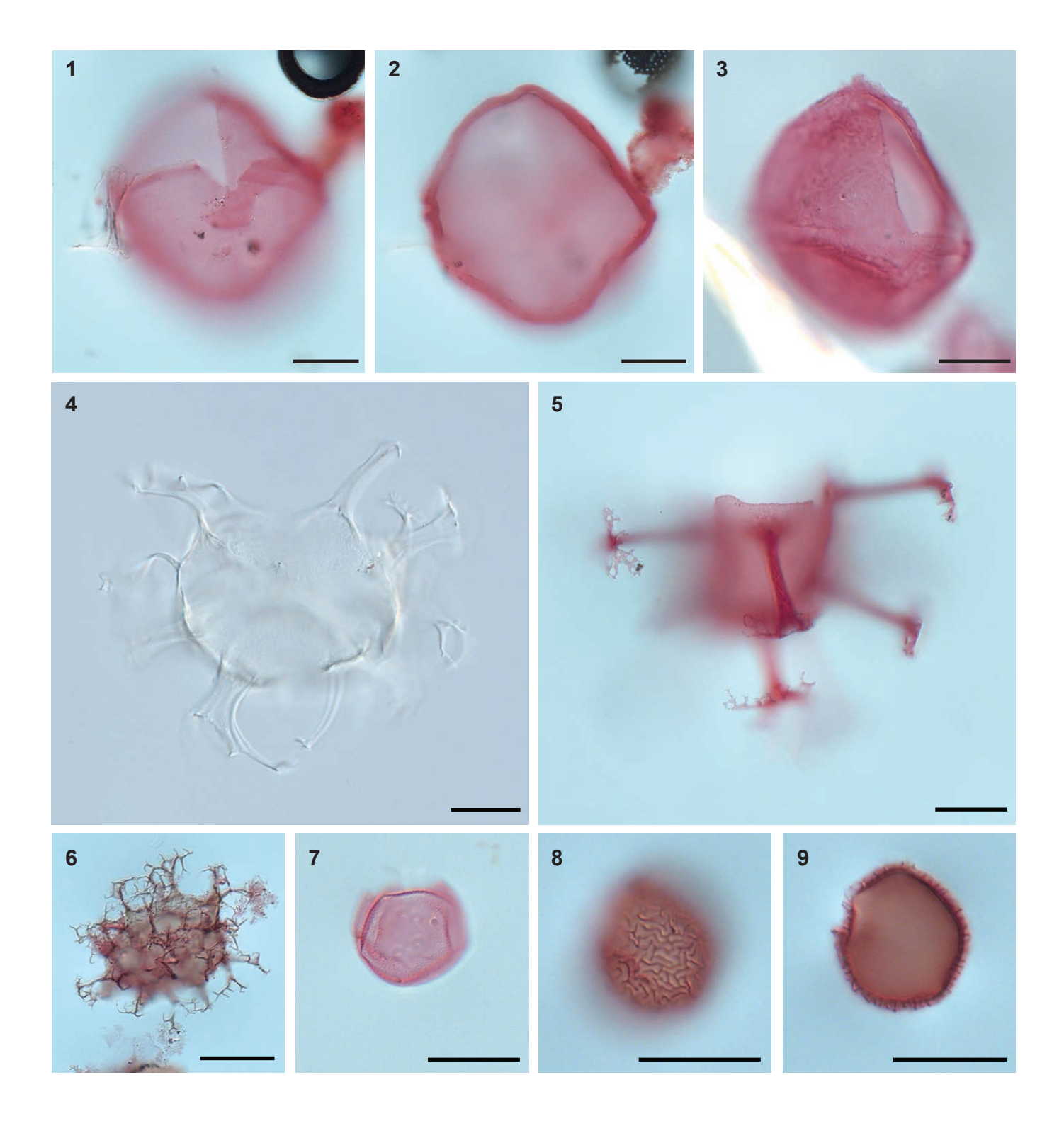


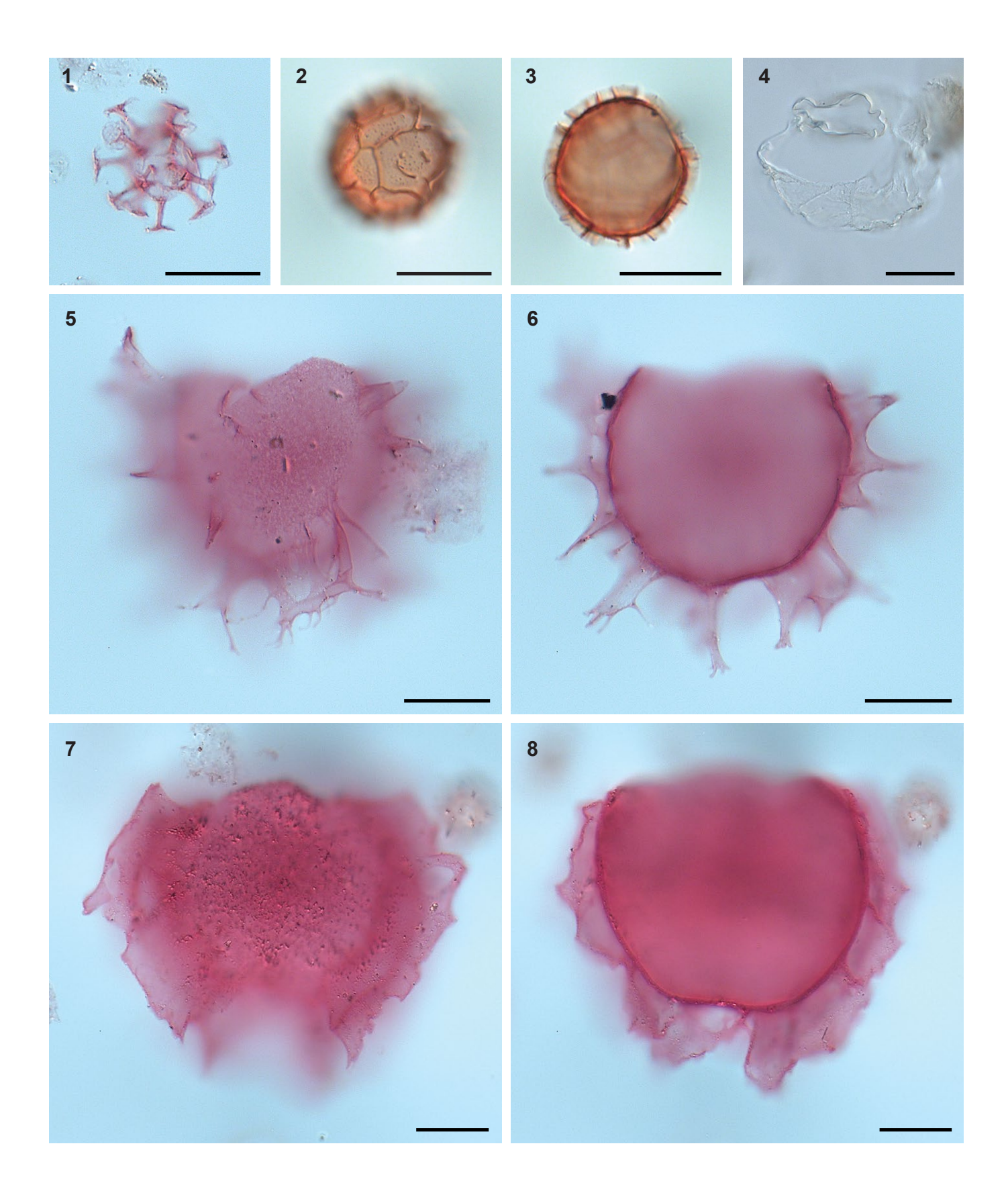
Fig. 5

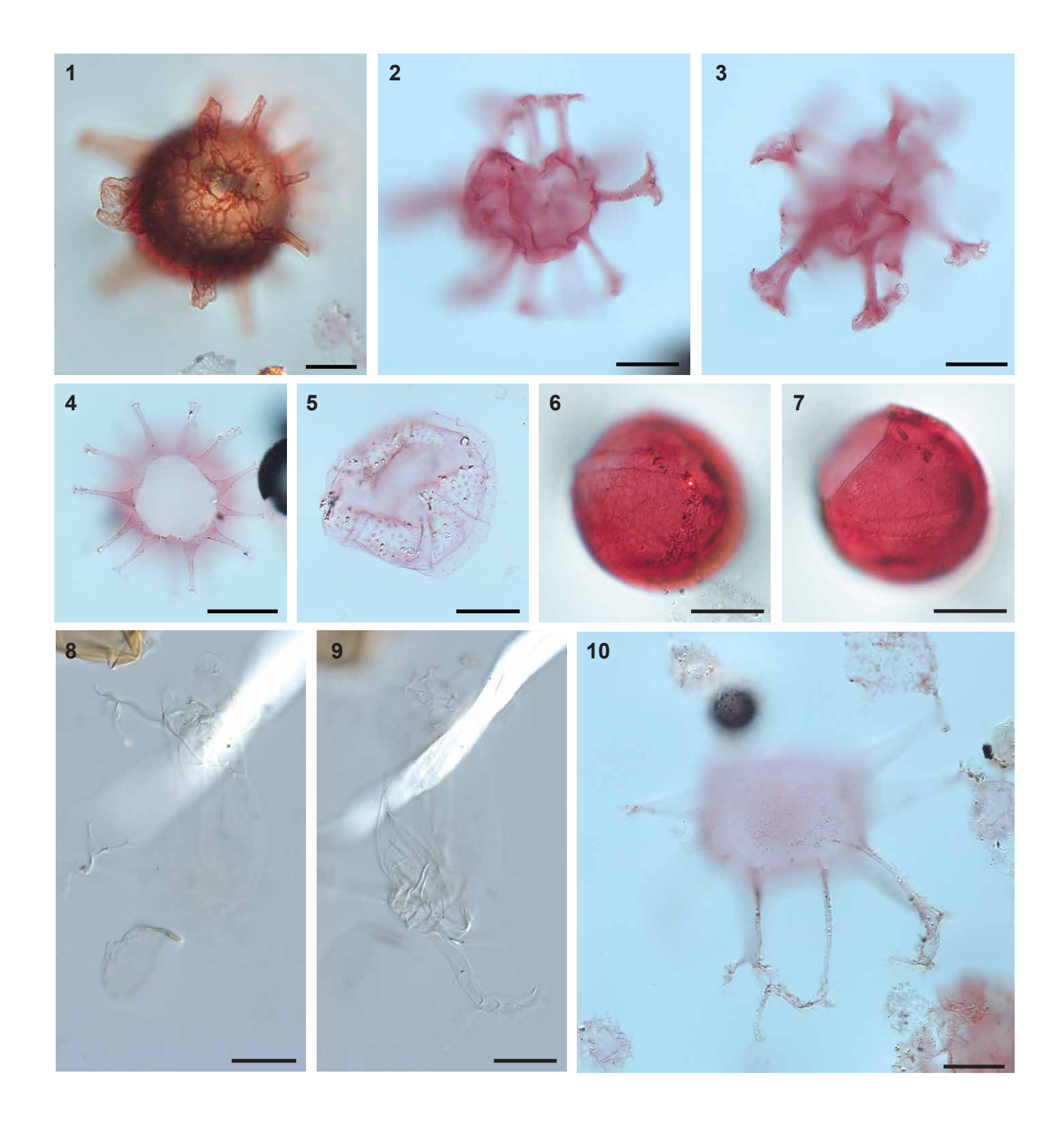


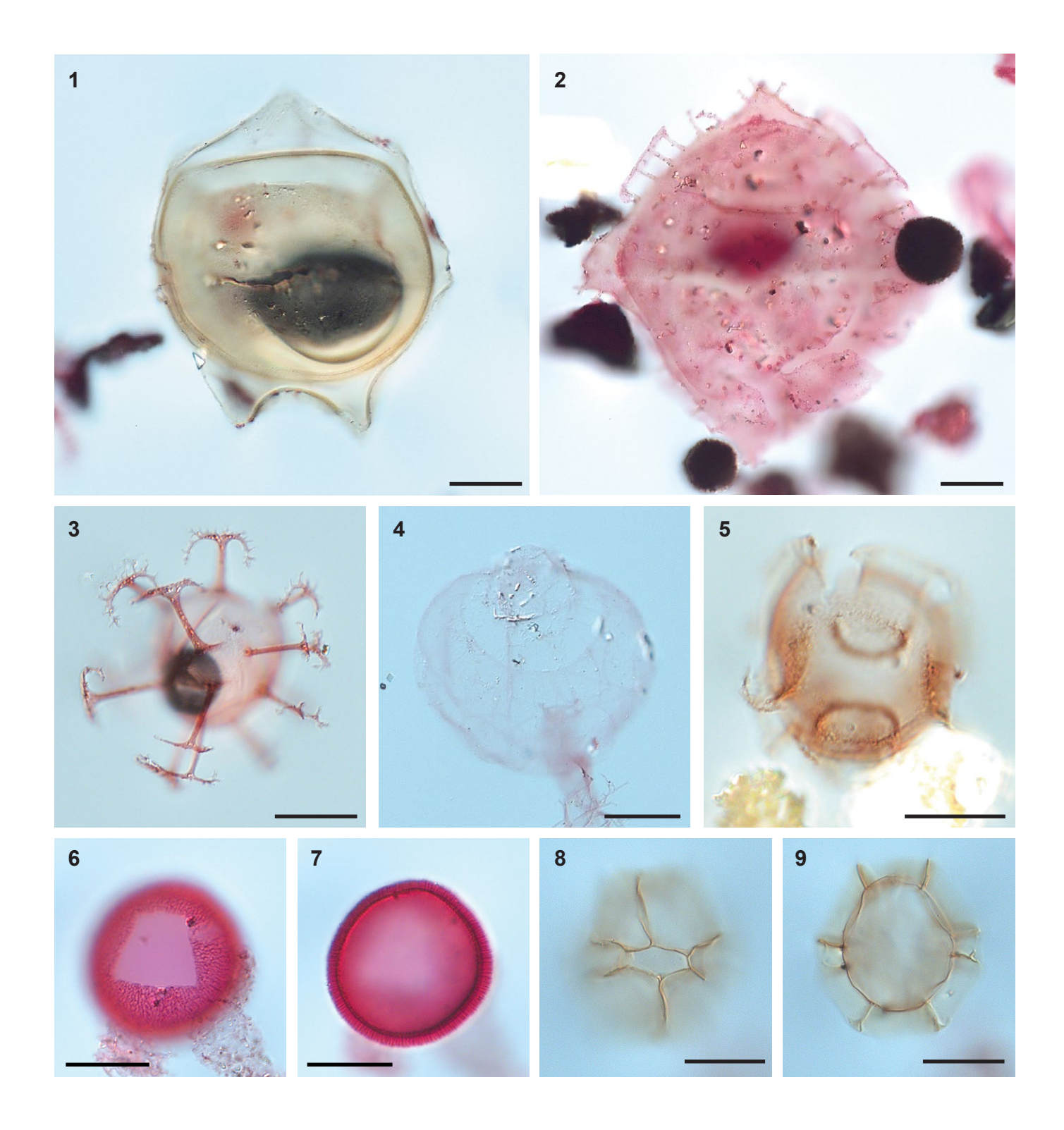


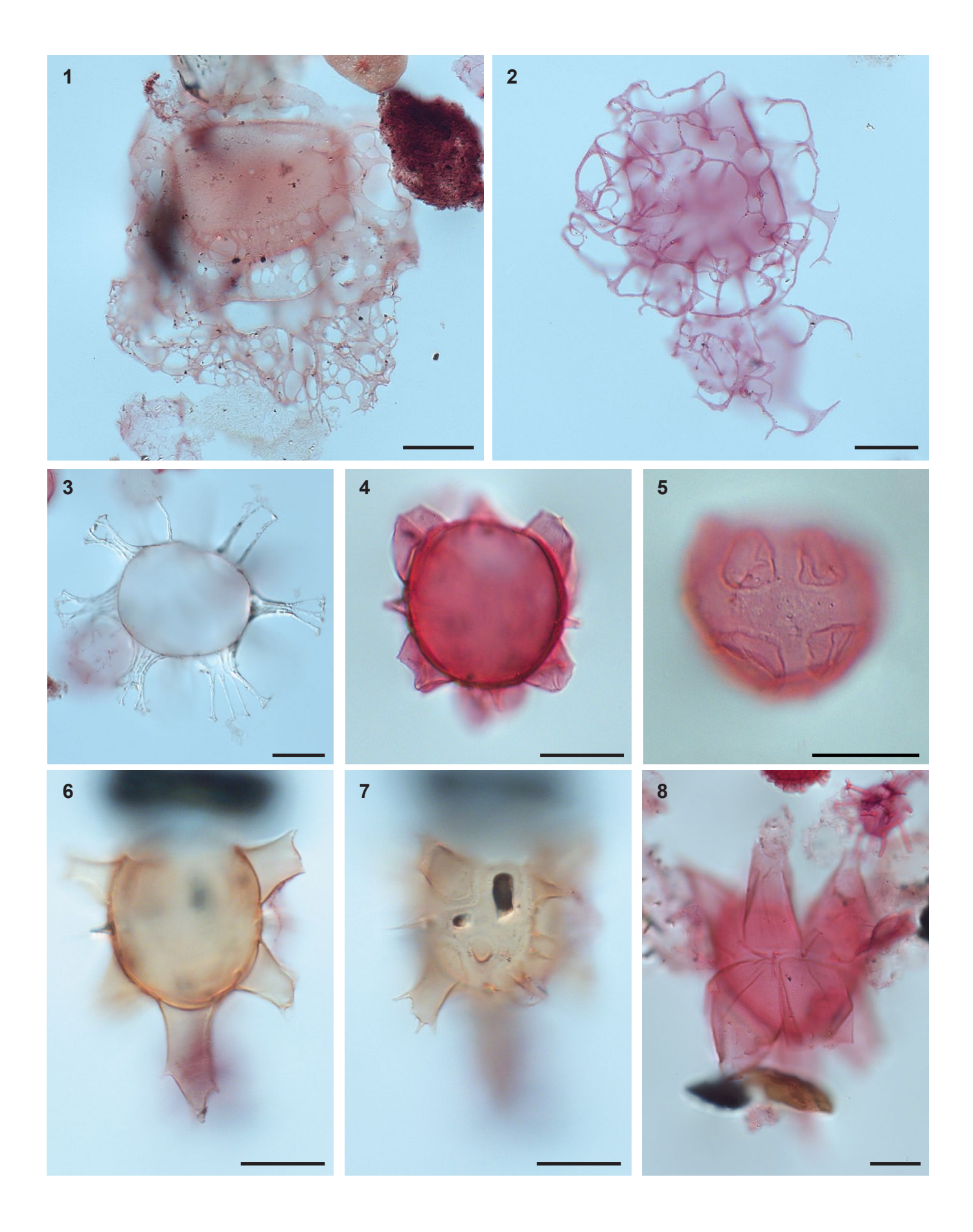


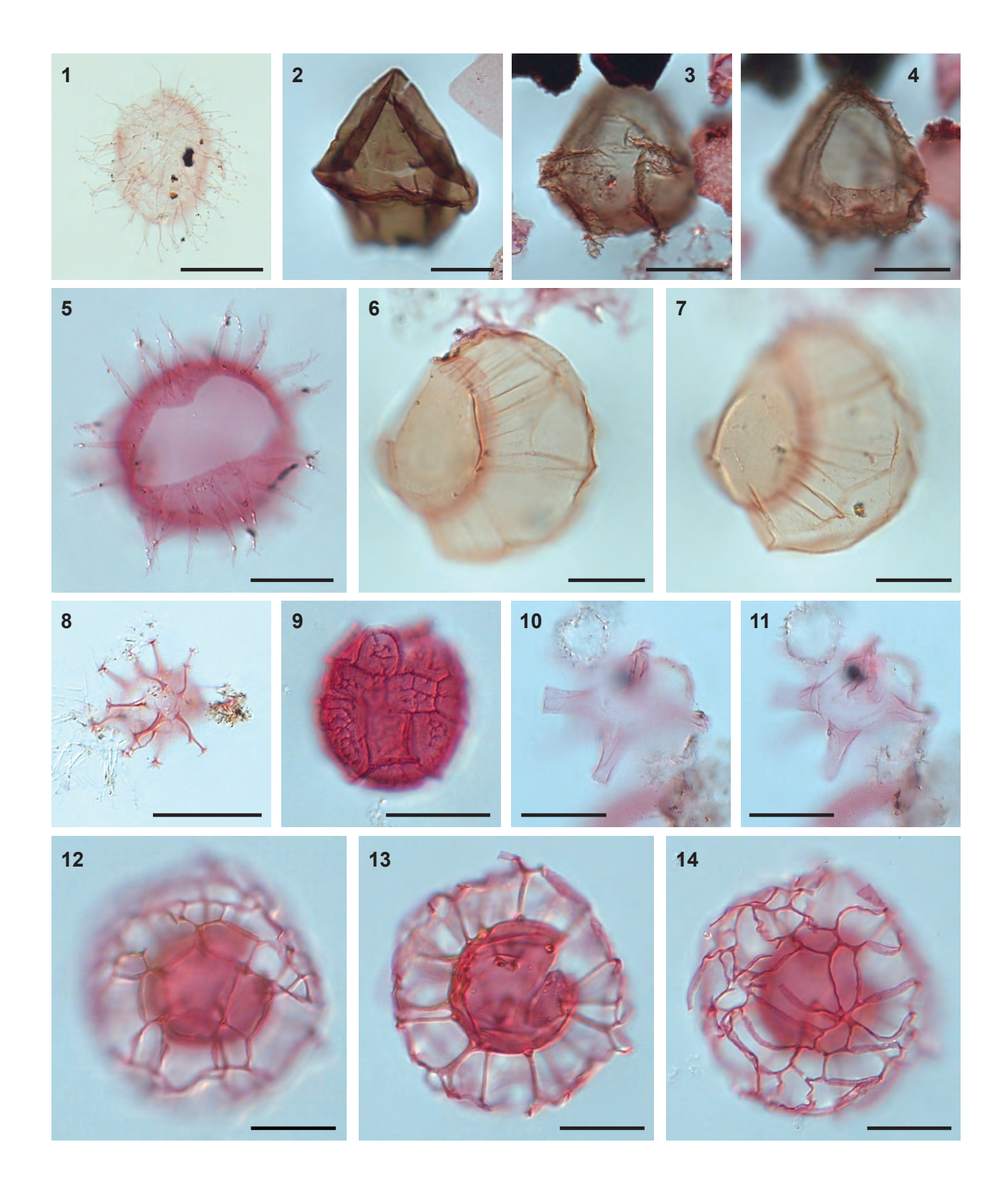


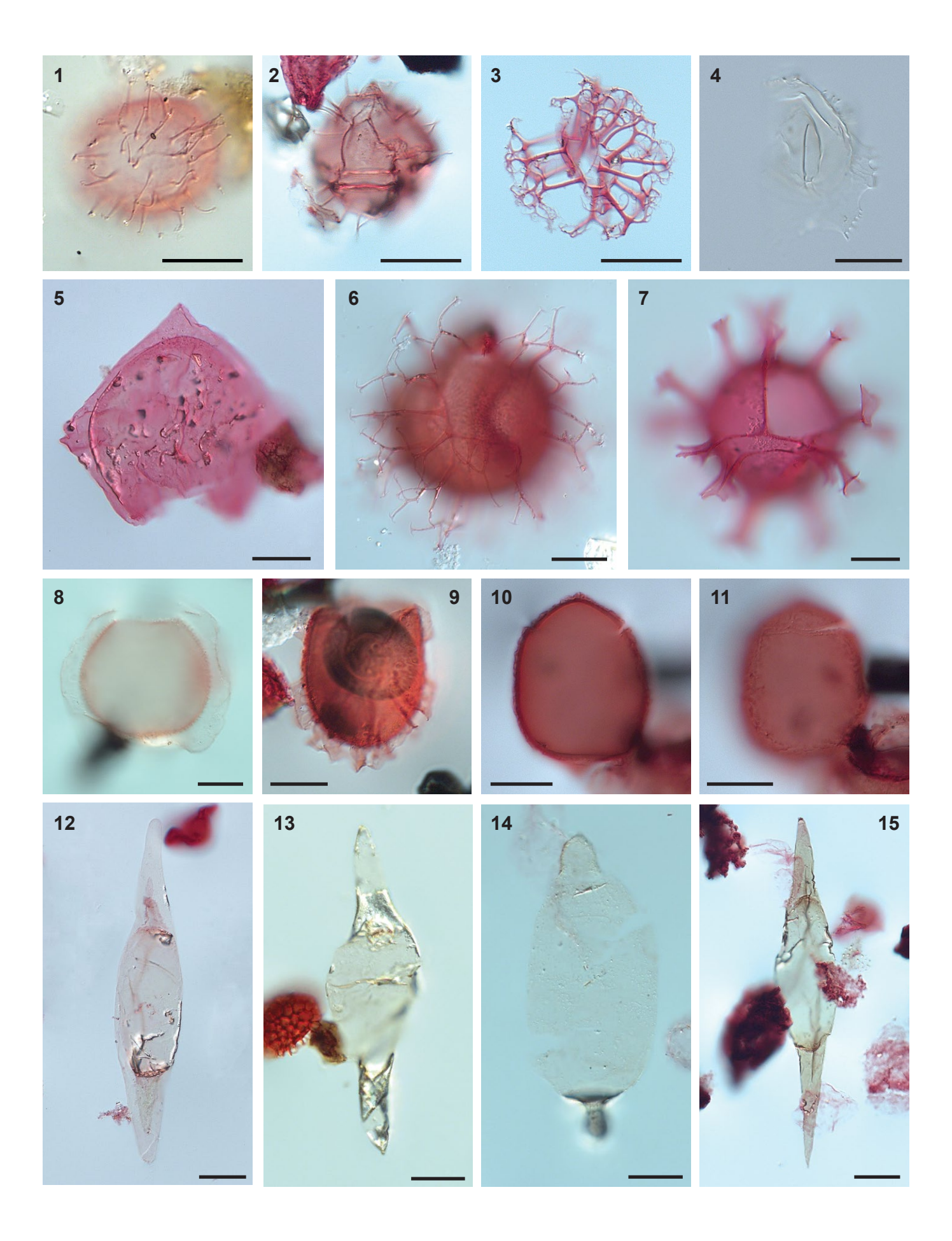












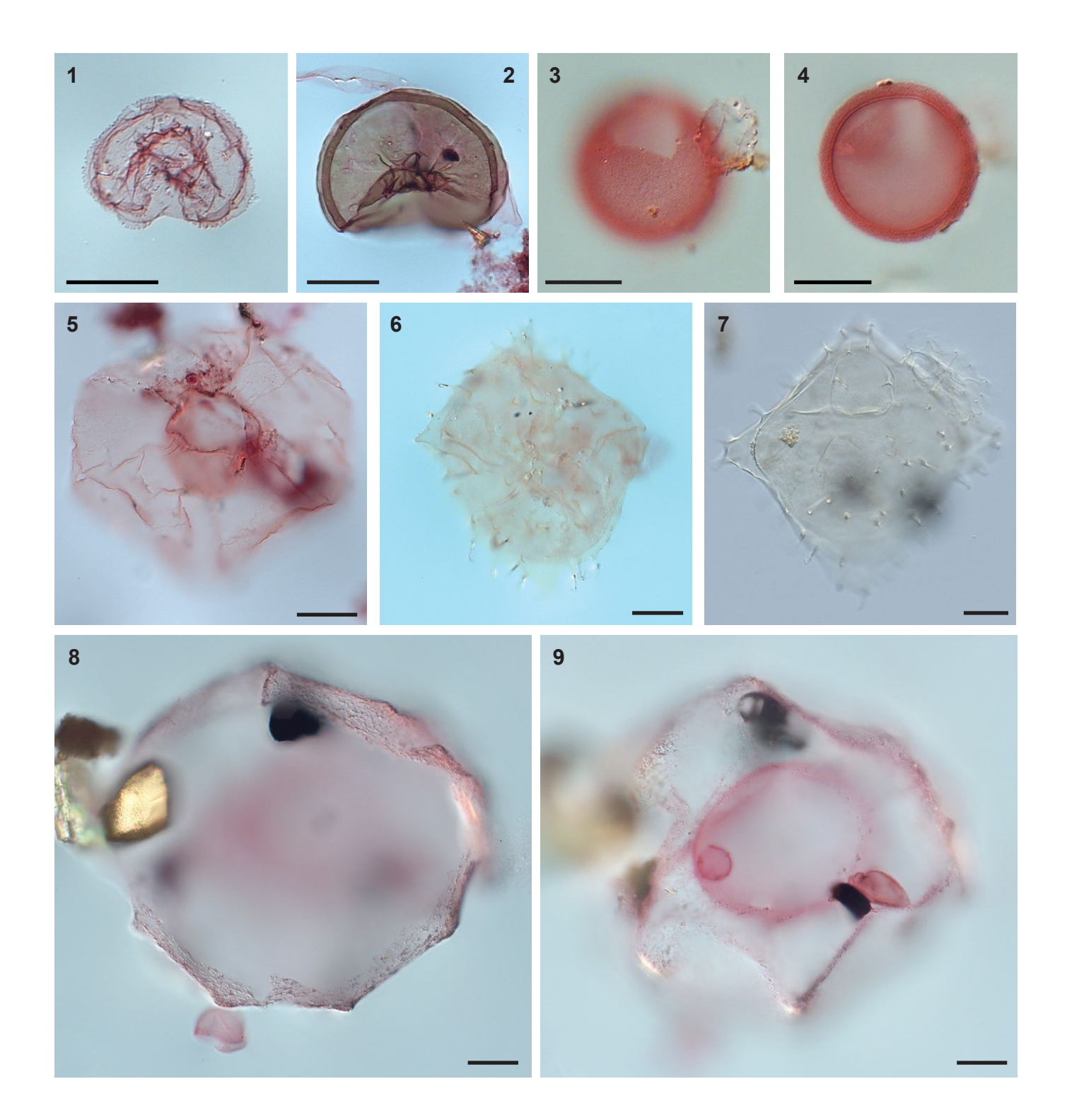


Table 1

			Age (Ma)		
Taxon	Newfound- land Drift Exp. 342	Norwegian -Greenland Sea	Norwegian Sea	North Sea/Danish land area	Umbria- Marche (Italy)
Artemisiocysta cladodichotoma	29.6				
Chiropteridium galea	30.5	33.5			
Oligokolpoma galeottii	30.5				31.3
Chiropteridium lobospinosum	32.0	33.5			32.5
Hystrichokolpoma pusillum	32.0				32.3
Melitasphaeridium asterium	33.5				
Filisphaera filifera	33.7				
Spiniferites manumii	33.7	33.0	31.4		
Svalbardella spp.	33.7	42.2			29,1
Lophocysta sulcolimbata	34.6		21,1		

Table 2

	Age (Ma)						
Taxon	Newfound- land Drift Exp. 342	Norwegian -Greenland Sea	Norwegian Sea	North Sea/Danish land area	Umbria-Marche (Italy)		
Svalbardella spp.	22.1	33.5	30.4		27.1		
Deflandrea spp.	22.2						
Filisphaera filifera	22.7						
Hystrichokolpoma pusillum	22.8				23.6		
Wetzeliella gochtii/symmetrica group	26.1				26.9 (W. gochtii)		
Areoligera semicirculata	26.6		30.4	C8r	27.4		
Saturnodinium pansum	26.6			C8r	24.5		
Enneadocysta pectiniformis	27.1				27.9		
Phthanoperidinium comatum	30.7				27.9		
Spiniferites manumii	31.7	30.8		C12r			
Lentinia serrata complex	33.3				32.4		
Stoveracysta sp. 1	33.5				30.9 (S. spp.)		
Areosphaeridium diktyoplokum	33.7	33.5		C12r	33.4		
Charlesdowniea clathrata	33.7				32.4		
Hemiplacophora semilunifera	33.8				33.6*		
Cordosph. cf. funiculatum	34.0						
Schematophora speciosa	34.1				34.5*		
Lophocysta sulcolimbata	34.6						

_	Key to range charts		Micro-		
Taxon	Fig. 3	Fig. 4	Fig. 5	Fig. 6	photographs
Achomosphaera spp.	7	8	12	9	1
Achilleodinium biformoides (Eisenack, 1954b) Eaton, 1976		59	2	27	
Apteodinium australiense (Deflandre and Cookson, 1955) Williams, 1978	33	5	39		Pl. I, Figs. 1-2
Apteodinium spiridoides Benedek, 1972		40		51	Pl. I, Fig. 3
*Areoligera semicirculata (Morgenroth, 1966b) Stover and Evitt, 1978		53	4		Pl. I, Fig. 4
Areoligera spp. (undiff.)		51	13		
*Areosphaeridium diktyoplokum (Klumpp, 1953) Eaton, 1971				35	Pl. I, Fig. 5
*Artemisiocysta cladodichotoma Benedek, 1972	26	45	51		Pl. I, Fig. 6
Batiacasphaera micropapillata Stover, 1977					Pl. I, Fig. 7
Batiacasphaera sphaerica Stover, 1977					
Batiacasphaera spp. (undiff.)	8	9	14	10	
Cerebrocysta bartonensis Bujak in Bujak et al., 1980		29	49	36	Pl. I, Figs. 8-9
*Charlesdowniea clathrata (Eisenack, 1938b) Lentin and Vozzhennikova, 1989				37	Pl. IV, Fig. 2
*Chiropteridium galea (Maier, 1959) Sarjeant, 1983	30	3	15		Pl. II, Figs. 5-6
*Chiropteridium lobospinosum Gocht, 1960	3	21	16		Pl. II, Figs. 7-8
Chiropteridium spp. (undiff).	32	52	17		
Cleistosphaeridium ancyreum (Cookson and Eisenack, 1965b) Eaton et al., 2001					
Cleistosphaeridium diversispinosum Davey et al., 1966	<u> </u>				1
Cleistosphaeridium spp. (undiff.)	9	10	18		DI III 51
Cordosphaeridium cantharellus (Brosius, 1963) Gocht, 1969	4	30	19	44	Pl. III, Figs. 2-3
*Cordosphaeridium cf. funiculatum of Biffi and Manum, 1988	-	 _	20	48	Pl. III, Fig. 1
Cordosphaeridium minimum (Morgenroth, 1966a) Benedek, 1972		7	20	12	Pl. II, Fig. 1
Cordosphaeridium spp. (undiff.)	1	36	21	11	DI II 5' 2 2
Corrudinium incompositum (Drugg, 1970b) Stover and Evitt, 1978		58		5	Pl. II, Figs. 2-3
Cribroperidinium sp. 1	-	62			Pl. III, Figs. 6-7
Cyclodictyon spp. Dapsilidinium pseudocolligerum (Stover, 1977) Bujak et al., 1980	6	62 11	22	14	Pl. II, Fig. 4
Dapsilidinium spp.	0	65	50	14	P1. III, FIg. 4
Deflandrea phosphoritica		03	30		Pl. IV, Fig. 1
Deflandrea spp. (undiff.)	36	12	23	15	11.1V,11g.1
Dinopterygium cladoides Deflandre, 1935	30	47	40	1	Pl. III, Fig. 5
Diphyes colligerum (Deflandre and Cookson, 1955) Cookson, 1965a		1,	-10		11.11,118.3
Distatodinium biffii Brinkhuis et al., 1992		48	52		Pl. III, Figs. 8-9
Distatodinium craterum Eaton, 1976					l
Distatodinium ellipticum (Cookson and Eisenack, 1965a) Eaton, 1976					
Distatodinium spp. (undiff.)		33	41	4	
*Enneadocysta pectiniformis (Eaton, 1971) Stover and Williams, 1995		57		16	Pl. IV, Fig. 3
Enneadocysta magna Fensome et al., 2006		61			Pl. III, Fig. 10
*Filisphaera filifera Bujak, 1984	37	1	24	52	Pl. IV, Figs. 6-7
Gelatia inflata Bujak, 1984	2	31	25	28	Pl. IV, Fig. 4
Glaphyrocysta intricata (Eaton, 1971) Stover and Evitt, 1978					
Glaphyrocysta semitecta (Bujak in Bujak et al., 1980) Lentin and Williams, 1981				38	Pl. V, Fig. 1
Glaphyrocysta spp. (undiff.)	38	37	42	39	Pl. V, Fig. 2
Hapsocysta kysingensis Heilmann-Clausen and Van Simaeys, 2005	27	34			
*Hemiplacophora semilunifera Cookson and Eisenack, 1965a				45	Pl. IV, Fig. 5
Heteraulacacysta porosa Bujak in Bujak et al., 1980		56		40	1
Heteraulacacysta pustulata Jan du Chêne and Adediran, 1985				41	
Heteraulacacysta spp. (undiff.)		43	46		1
Homotryblium plectilum Drugg and Loeblich Jr., 1967	12	2	7	29	Pl. V, Fig. 3
Hystrichokolpoma cinctum Klumpp, 1953		<u> </u>	_		Pl. V, Fig. 8
*Hystrichokolpoma pusillum Biffi and Manum, 1988	39	27	5		Pl. V, Fig. 4
Hystrichokolpoma rigaudiae Deflandre and Cookson, 1955	13	22	11	30	Pl. V, Figs. 6-7
Hystrichokolpoma salacia Eaton, 1976		-			
Hystrichokolpoma sp. sensu Biffii and Manum 1988	-	-			+
Hystrichokolpoma truncata Biffi and Manum, 1988	10	12	26	17	1
Hystrichokolpoma spp. (undiff.)	14	13	26	17	+
Hystrichokolpoma/Oligokolpoma spp.		60	6		+
Hystrichosphaeropsis obscura Habib, 1972		-			1
Impagidinium dispertitum (Cookson and Eisenack, 1965a) Stover and Evitt, 1978	-	-			+
Impagidinium maculatum (Cookson and Eisenack 1001h) Staver and Evitt 1070	i		ļ		
Impagidinium maculatum (Cookson and Eisenack, 1961b) Stover and Evitt, 1978			l		
Impagidinium paradoxum (Wall, 1967) Stover and Evitt, 1978					
	15	38	43	18	

Appendix, Table A.1

Impletosphaeridium insolitum Eaton, 1976	17	23	28		Pl. VI, Fig. 1
Lejeunecysta fallax (Morgenroth, 1966b) Artzner and Dörhöfer, 1978					Pl. VI, Fig. 2
Lejeunecysta hyalina (Gerlach, 1961) Artzner and Dörhöfer, 1978					
Lejeunecysta spp.	18	15	44	20	
*Lentinia serrata Bujak in Bujak et al., 1980		41		33	Pl. VI, Figs. 3-4
Lingulodinium machaerophorum (Deflandre and Cookson, 1955) Wall, 1967	19	24	29	7	Pl. VI, Fig. 5
*Lophocysta sulcolimbata Manum, 1979				46	Pl. VI, Figs. 6-7
*Melitasphaeridium asterium (Eaton, 1976) Bujak et al., 1980	20	4	30	2	Pl. VI, Fig. 8
Microdinium reticulatum Vozzhennikova, 1967		58		5	Pl. VI, Fig. 9
Nematosphaeropsis reticulensis (Pastiels, 1948) Sarjeant, 1986					, , ,
Nematosphaeropsis labyrinthus (Ostenfeld, 1903) Reid, 1974					Pl. VI, Figs. 12-14
Nematosphaeropsis spp. (undiff.)	21	16	45	21	,go: == =:
*Oligokolpoma galeottii Pross et al., 2010	31	28	1		Pl. VI, Figs. 10-11
Oligokolpoma spp.					Pl. V, Fig. 5
Operculodinium centrocarpum (Deflandre and Cookson, 1955) Wall, 1967	22	17	31	22	Pl. VII, Fig. 1
Operculodinium spp. (undiff.)	28	6	32	49	1,g
Palaeocystodinium golzowense Alberti, 1961	23	18	33	23	
Palaeocystodinium spp. (undiff.)		44	34		Pl. VII, Fig. 15
Pentadinium laticinctum Gerlach, 1961		42	1		Pl. VII, Fig. 8
Pentadinium spp. (undiff.)		49	35		11. VII, 11g. 0
Phthanoperidinium amoenum Drugg and Loeblich Jr., 1967		63	33		
*Phthanoperidinium comatum (Morgenroth, 1966b) Eisenack and Kjellström, 1972		66		24	Pl. VII, Fig. 2
Phthanoperidinium filigranum (Benedek, 1972) Benedek and Sarjeant, 1981		00		24	Fi. VII, Fig. 2
Phthanoperidinium geminatum Bujak in Bujak et al., 1980		64			
Phthanoperidinium spp. (undiff.)	24	19		3	
Polysphaeridium spp. (unum.)	29	39	47	3	
· · · · · · · · · · · · · · · · · · ·	5		 	25	DI VIII Eia 2
Reticulatosphaera actinocoronata Benedek, 1972	5	20	36	25 42	Pl. VII, Fig. 3
Rhombodinium draco Gocht, 1955		Γ1	8	42	Pl. VII, Fig. 5
*Saturnodinium pansum (Stover, 1977) Brinkhuis et al., 1992		54	•		Pl. VII, Fig. 4
*Schematophora speciosa Deflandre and Cookson, 1955				50	Pl. VII, Fig. 9
Selenopemphix crenata Matsuoka and Bujak, 1988					Pl. VIII, Fig. 1
Selenopemphix nephroides Benedek, 1972	40	45		20	Pl. VIII, Fig. 2
Selenopemphix spp. (undiff.)	18	15	44	20	DI VIII EL C
*Spiniferites manumii (Lund, 2002) Schiøler 2005		67		31	Pl. VII, Fig. 6
Spiniferites pseudofurcatus (Klumpp, 1953) Sarjeant, 1970		35	9	8	Pl. VII, Fig. 7
Spiniferites spp. (undiff.)	7	8	12	9	51.141.51.40.44
*Stoveracysta sp. 1			0.7	34	Pl. VII, Figs. 10-11
*Svalbardella spp.	35	25	37	32	Pl. VII, Figs. 12-14
Tectatodinium pellitum Wall, 1967	25	32	38	26	Pl. VIII, Figs. 3-4
Thalassiphora delicata Williams and Downie, 1966c					Pl. VIII, Fig. 5
Thalassiphora fenestrata Liengjaren et al., 1980					Pl. VIII, Fig. 8
Thalassiphora gracilis Heilmann-Clausen and Van Simaeys, 2005					
Thalassiphora pelagica (Eisenack, 1954b) Eisenack and Gocht, 1960		50	10	47	Pl. VIII, Figs. 9-10
Thalassiphora spp. (undiff.)		55	3	43	
*Wetzeliella gochtii Costa and Downie, 1976		46	48	6	Pl. VIII, Fig. 6
*Wetzeliella symmetrica Weiler, 1956		46	48	6	Pl. VIII, Fig. 7
undiff. dinocysts	40	68	53	53	
indeterminate dinocysts	41	69	54	54	
*dinocysts used for biostratigraphy					